https://doi.org/10.1021/acs.inorgchem.6b02553

Novel Antitumor Platinum(II) Conjugates Containing the Non-steroidal Anti-inflammatory Agent Diclofenac: Synthesis and Mechanisms of Antiproliferative Effects

Francesco Paolo Intini,[†,§] Juraj Zajac,[⊥,‡,§] Vojtech Novohradsky,[⊥] Teresa Saltarella,[†] Concetta Pacifico,[†] Viktor Brabec,[⊥,‡] Giovanni Natile,*[,†] and Jana Kasparkova*[,⊥]

[†]Department of Chemistry, University of Bari "Aldo Moro", 70125 Bari, Italy

[⊥]Institute of Biophysics, Academy of Sciences of the Czech Republic, Kralovopolska 135, 61265 Brno, Czech Republic

[‡] Department of Biophysics, Faculty of Science, Palacky University, Slechtitelu 27, 78371 Olomouc, Czech Republic

ABSTRACT: Diclofenac (DCF) is a potent non-steroidal anti-inflammatory drug exhibiting antitumor effects. We present new Pt(II) derivatives of cisplatin containing DCF ligand(s) as potent cytotoxic agents including activity in a cisplatin resistant line and the COX-2 positive tumor cell lines. One of these compounds, compound **3**, in which DCF molecules are coordinated to Pt(II) through their carboxylic group, is markedly more potent than its congeners in which DCF ligands are conjugated to Pt(II) via a diamine. The potency of this compound is due to several factors including enhanced internalization that correlates with enhanced DNA binding and cytotoxicity. Mechanistic studies show that **3** combines multiple effects. After its accumulation in the cell, it releases DCF ligands upon intracellular hydrolysis, which affects distribution of cells in individual phases of the cell cycle, inhibits glycolysis and/or lactate transport, collapses mitochondrial membrane potential and suppresses the cellular properties characteristic for metastatic progression.

INTRODUCTION

Non-steroidal anti-inflammatory drugs (NSAIDs) are frequently used as analgesics, anti-inflammatories and antipyretics.[1] Several studies have shown that the influences of NSAIDs are essentially based on the inhibition of the cyclooxygenase enzyme system (COX) that is involved in the conversion of arachidonic acid to prostaglandins, prostacyclin, and thromboxane.[2-5] Several recent *in vitro* and *in vivo* studies have also reported chemopreventive and chemotherapeutic effects of NSAIDs. In addition, clinical trials demonstrated that NSAIDs cause the regression of pre-existing adenomas in patients with familial adenomatous polyposis, and prevent the development of colon tumors in carcinogen-treated animals.[6-9] Studies on colorectal carcinomas have also shown that COX inhibitors reduce tumor growth and angiogenesis by inhibiting expression of pro-angiogenic factors (such as vascular endothelial growth factor) which are frequently over-expressed.[10]

Notably, the NSAIDs, such as indomethacin, ibuprofen, and aspirin, exhibit antitumor activity only at relatively high (milimolar) concentrations, which limits their pharmacological applications as antitumor drugs.[10-13] This is so because at neutral pH these NSAIDs are monoanionic and therefore do not efficiently accumulate in tumor cells. Recently, various NSAIDs were used as ligands in derivatives of metal-based drugs. Examples are derivatives of ruthenium(II)- or osmium(II)-*p*-cymene complexes[14] and Pt(II) or Pt(IV) derivatives of antitumor cisplatin or oxaliplatin.[13, 15, 16] Notably, the presence of NSAID ligands in Pt(II) or Pt(IV) conjugates renders these derivatives of cisplatin or oxaliplatin hydrophobic. Consequently, due to the higher lipophilicity of these conjugates their transport across cell membranes is facilitated. Thus, they efficiently accumulate in tumor cells treated with these agents already at concentrations more than three orders of magnitude lower (micromolar) than those required from free NSAIDs. The design of these Pt-NSAID conjugates was based on the premise that attaching NSAIDs to the derivatives of cisplatin or oxaliplatin should result in simultaneous release inside the cell of two antiproliferative agents that act by different mechanisms on different cellular targets. Thus, the platinum conjugates could also serve to bring into the tumor cells, along with the free antitumor Pt(II) compound, also free NSAIDs in the amount that could make it possible to execute their biological function.

Prior studies described cisplatin analogues conjugated with NSAIDs indomethacin and ibuprofen.[12, 15] Although these conjugates are potent COX inhibitors, they appear to execute their cytotoxic action via COX-independent mechanisms. The increased lipophilicity and kinetic inertness of these conjugates have been proposed to facilitate the cellular accumulation of the active platinum drugs. Other papers reported Pt(IV) prodrugs of cisplatin containing as axial ligands another NSAID, namely aspirin, which was shown to exhibit anti-inflammantory and antineoplastic effects.[13, 16, 17] The results showed that aspirin was released intracellularly from the Pt(IV) prodrug by its reduction. The release was observed when the tumor cells were treated with the Pt(IV) prodrug only at micromolar concentrations and the amount of released aspirin was sufficient to modulate the cellular response to the platinum agent; apparently the apoptosis was promoted via the BCL-2 associated mitochondrial pathway.[16]

Diclofenac, sodium {2-[(2,6-dichlorophenyl)amino]phenyl}acetate (DCF, Figure 1), is a potent NSAID of the phenylalkanoic acids group.[18] In addition to the antitumor effect attributed to the inhibition of COX, DCF has also shown novel COX-independent effects caused by its influencing of the mitochondrial activity.[19] The reduction in mitochondrial activity might contribute to the anti-proliferative effect of DCF on tumor cells. It was demonstrated that DCF targets tumor cell proliferation by causing the inhibition of both the transcription factor MYC and the lactate transporters.[19] Interestingly, so far no other NSAIDs have been shown to affect glucose metabolism. Moreover, it was observed that DCF stimulates basal and uncoupled respiration, inhibits ATP synthesis, and collapses membrane potential in mitochondria.[20]

Platinum(II) compounds are used in 50% of all cancer therapies[21] and, among these, cisplatin (Figure 1), carboplatin, and oxaliplatin are used worldwide.[22, 23] Their use is however limited by

side effects and acquired resistance.[24] To improve the activity of existing platinum drugs, explored strategies contemplate, among others, targeting platinum drugs to cancer cells and combining platinum drugs with other therapeutic agents. Thus, constructs containing both a cisplatin-like compound and another moiety acting synergistically with cisplatin have been employed.

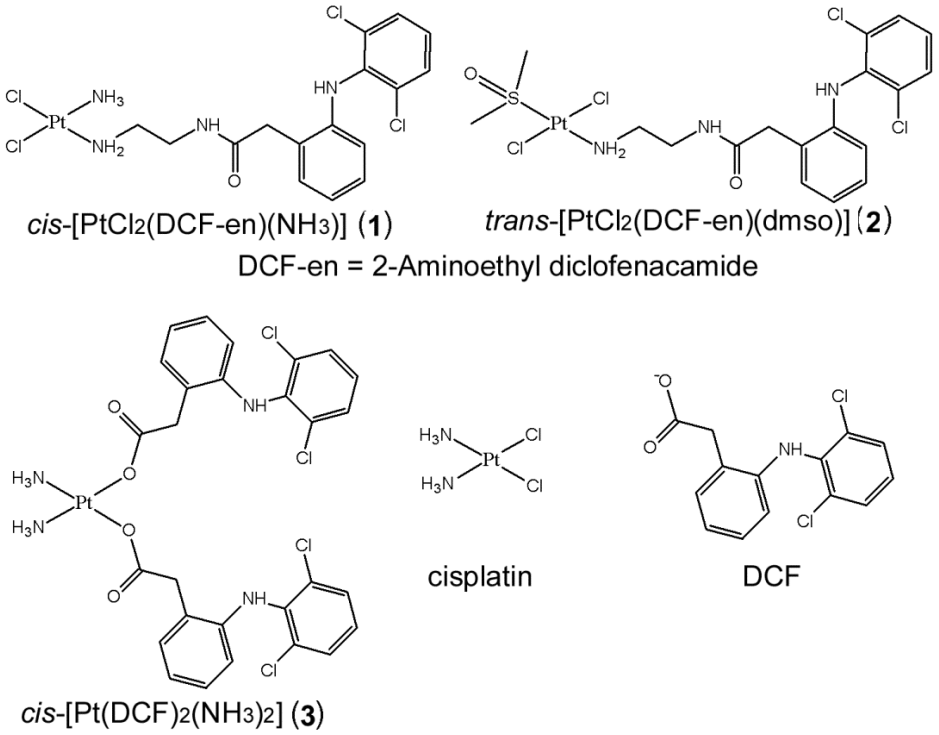

Figure 1. Derivatives of cisplatin with diclofenac (DCF) studied in this work.

With the aim to shed light on the mode of action of Pt(II)-NSAID pro-drugs, and optimizing the choice of NSAID ligands, we have synthesized and investigated the biological activity of Pt(II) derivatives of cisplatin containing DCF ligand(s) with various intracellularly cleavable linkers. Conjugation of DCF to platinum (compounds **1** and **2**, Figure 1) was achieved via a diamine that can coordinate to platinum with one end and link DCF with a peptidic bond at the other end. The peptidic bond is stable under neutral conditions, but may be cleaved in the acidic environment of the lysosome or endosome after uptake of the conjugate into the cells. Furthermore, the amidic bond can also undergo enzymatic hydrolysis by peptidases or proteases. Compounds **1** and **2** were designed to release one molecule of DCF along with an antitumor-active platinum complex containing two chloride ligands as leaving ligands. Besides conjugation at the non-leaving ligand, DCF molecules were also coordinated to Pt(II) through their carboxylic group (compound **3**, Figure 1). Dissociation of the carboxylic ligands from the platinum(II) center of compound **3** inside the tumor cell can then take place in a similar way as activation of carboplatin.[25-27] The released parental DCF molecules should be able to carry out their biological functions and the $[Pt(NH_3)_2(OH_2)_2]^{2+}$ moiety should be able to interact with its key target (nuclear DNA).

RESULTS AND DISCUSSION

Synthesis and Characterization of *cis*-[PtCl$_2$(DCF-en)(NH$_3$)] (1) and *trans*-[PtCl$_2$(DCF-en)(DMSO)] (2). A possible approach to the synthesis of DCF-Pt(II) derivatives consists in the

derivatization of DCF with a diamine-linker to obtain a primary amine able to coordinate to the electrophilic platinum(II) center. By this approach more water soluble Pt(II) complexes could be obtained and the DCF moiety would be released upon hydrolysis of the amidic bond. For this purpose, we selected 1,2-ethylendiamine. Addition of 1,2-ethylendiamine to a chloroform solution of DCF imidazolide at room temperature affords 2-aminoethyldiclofenacamide (DCF-en) in good yield (shown in Scheme 1 together with the numbering scheme). The use of chloroform avoids the formation of the cyclic lactone as by-product.

DCF-en,

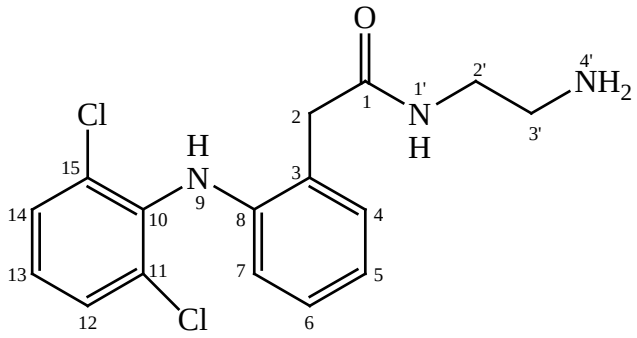

Scheme 1

The ligand was characterized by NMR, ESI-MS and elemental analysis. The spectroscopic and spectrometric features were in accord with the proposed formulation.

The ^{1}H-NMR spectrum of DCF-en in DMSO-d_6 (Figure 2, numbering of protons as in Scheme 1) shows: two signals falling at 8.45 and 8.33 ppm belonging to aminic (N9*H*) and amidic (N1'*H*) protons, respectively; five signals between 7.8 and 6.0 ppm due to aromatic protons, one singlet falling at 3.57 ppm belonging to the methylene protons of DCF, a multiplet at 3.06 and, finally, a triplet at 2.57 ppm belonging to the two methylenes of the diamine linker. The broad signal close to 1.50 ppm belongs to NH_2.[28] Similar values were previously reported for DCF-en, except for the NH_2 signal which was placed at 8.34 ppm.[29]

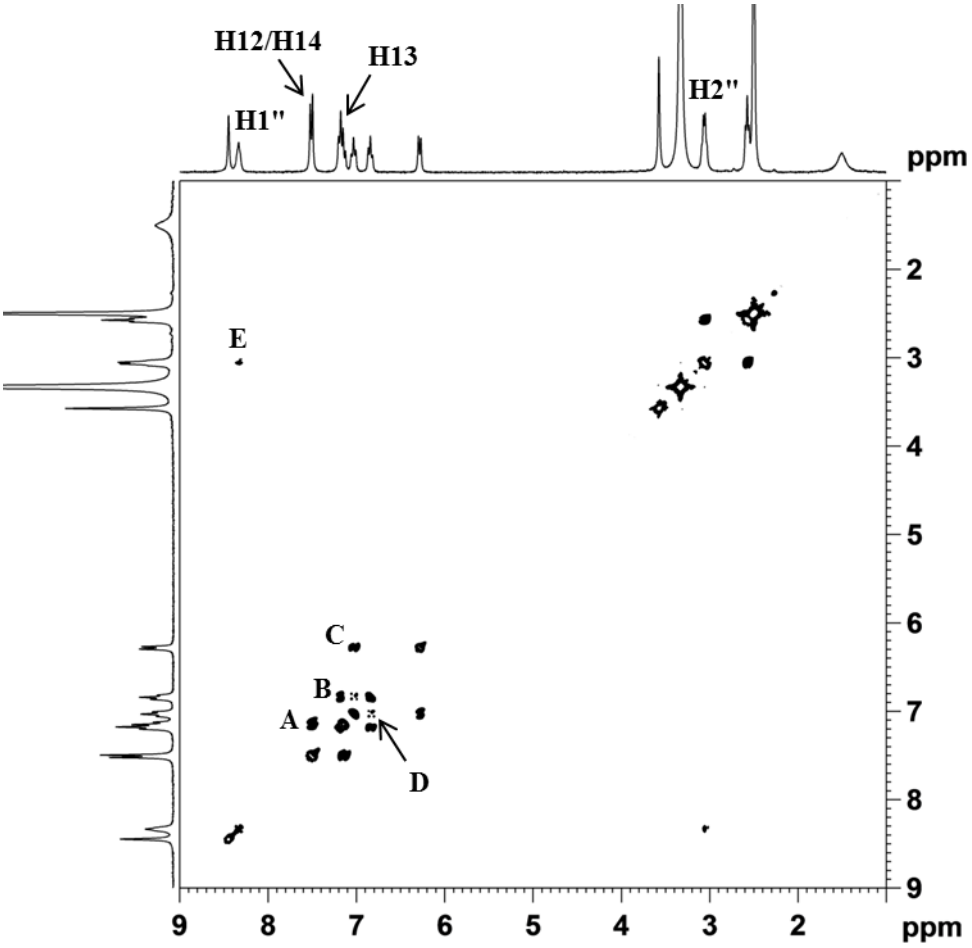

Figure 2. 1D and 2D COSY ^{1}H NMR spectra of DCF-en in DMSO-d_6.

The assignment of the aromatic protons was performed via a 2D COSY spectrum recorded in DMSO-d_6 (Figure 2). The spectrum shows a cross-peak (A) between the two signals falling at 7.51 and 7.15 ppm which, consequently, are assigned to protons C12/14*H* and C13*H*, respectively. A second cross peak (B) correlates the two signals falling at 7.18 and 6.85 ppm; the signal at 6.85 ppm has a cross peak (C) with the signal at 7.00 ppm and this latter has a cross peaks (D) with the signal falling at 6.28 ppm. Therefore these signals were assigned to C4*H*, C5*H*, C6*H* and C7*H*, respectively. Finally, the spectrum shows a cross peak I between the two signal falling at 8.33 and 3.06 ppm which were assigned to N1'H and C2'H_2, respectively. The multiplets falling at 3.06 and 2.58 ppm have chemical shifts typical for methylene groups linked to amidic and aminic nitrogens, respectively.[29]

This assignment was also supported by two NOESY cross-peaks (a and a' in Figure 3) between the signal at 8.33 ppm and the signals assigned to the methylene protons C2H_2 and C2'H_2.

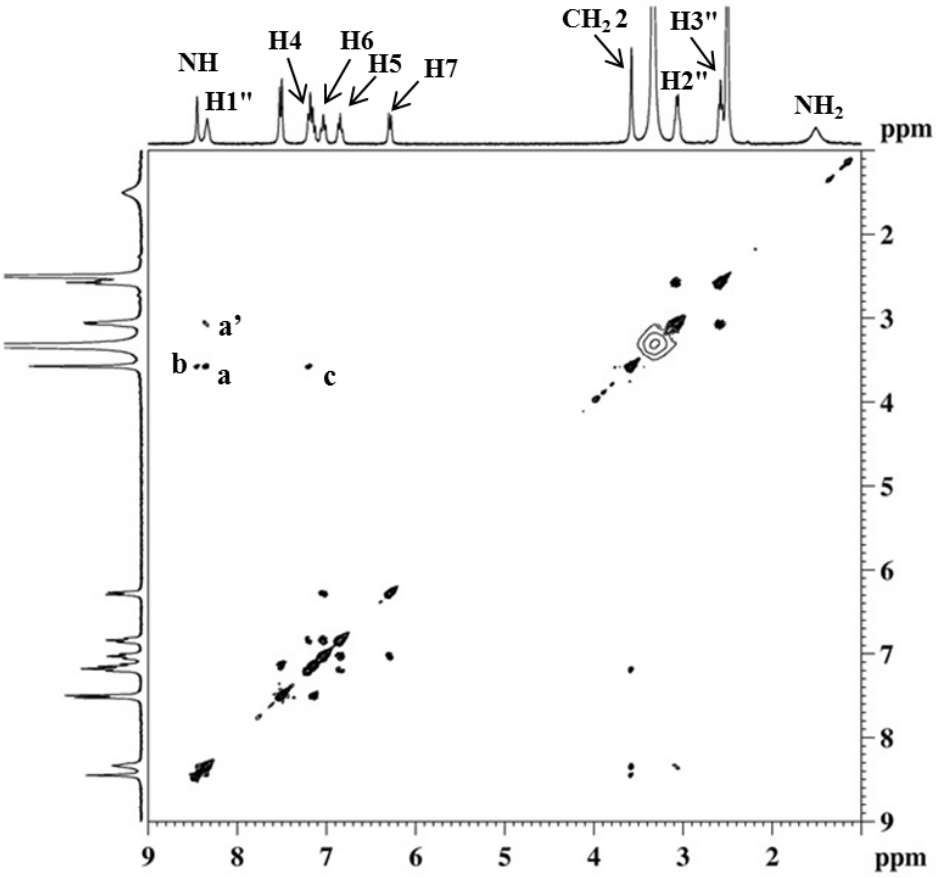

Figure 3. 1D and 2D NOESY ^{1}H NMR spectra of DCF-en in DMSO-d_6.

Moreover it was possible to assign the most deshielded signal (centered at 8.45 ppm) to the aminic proton C9*H* because of its spatial correlation (NOESY cross-peak b) with the singlet at 3.57 ppm (C2H_2). Finally, a NOESY cross-peak (cross peak c) correlates the last signal at 3.57 ppm (C2H_2) to the aromatic proton C4*H*. The triplet at 6.85 ppm, having a COSY cross-peak with proton C4*H*, was assigned to proton C5*H*. Finally, the remaining doublet and triplet were assigned to protons C7*H* and C6*H*, respectively. NMR data are summarized in Table 1S.

The synthesis of *cis*-[$PtCl_2$(DCF-en)(NH_3)] (**1**) was accomplished in CH_2Cl_2 starting from K[$PtCl_3(NH_3)$] and DCF-en (Scheme 2). The use of tetraphenylphosphonium chloride was required for enhancing the solubility of the platinum salt in a non-aqueous solvent. Compound **1** was insoluble in CH_2Cl_2 and could be isolated by filtration of the reaction mixture.

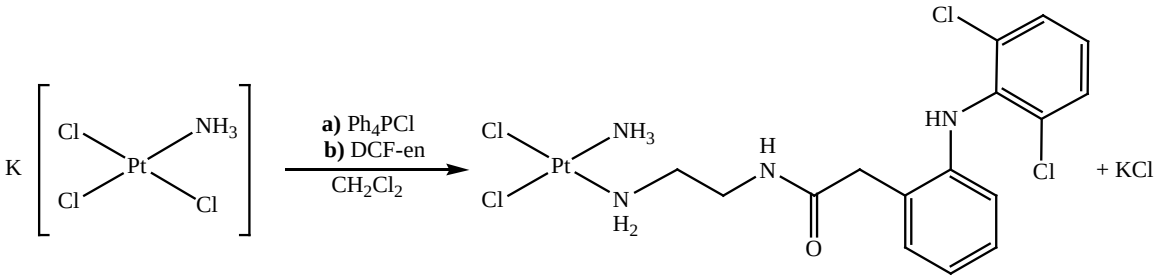

Scheme 2

The *cis* geometry of compound **1** is dictated by the reactivity of the starting substrate. In [$PtCl_3(NH_3)]^-$, the chloride *trans* to NH_3 is less reactive than the two □hloride ligands *cis* to NH_3

because of the lower *trans*-effect of the ammine as compared to that of a chloride ligand; as a consequence the DCF-en ligand displaces one of the two chloride ligands *cis* to NH_3 leading to a reaction product having *cis* geometry. Also in this case, the characterization has been based on elemental analyses, IR, ESI-MS, and NMR spectroscopy which allowed the assignment of all resonances.

The ^{1}H-NMR spectrum of complex **1** in DMSO-d_6 (Supporting Information, Figure S1) shows: two signals falling at 8.47 and 8.31 belonging to amidic (N1'*H*) and aminic (N9*H*) protons, respectively; five signals between 7.6 and 6.2 ppm due to aromatic protons, two signals between 5 and 3.7 ppm assigned to aminic protons of the diamine linker (N4'*H*) and NH_3 ligand, respectively. Finally, in the aliphatic region, there are three signals belonging to methylene protons of DCF and diamine linker. The assignment of all protons was carried out by 2D COSY and 2D NOESY experiments (not shown) and was in accordance with that of the free ligand (Supporting Information, Table S1).

The coordination to the metal center of the primary aminic nitrogen atom was confirmed by the deshielding of the corresponding protons with respect to the free ligand (1.50 ppm downfield). The second largest shifts, with respect to the free ligand, were observed for C2'H_2 (0.28 ppm) and *C3*' (4.3 ppm). All other DCF-en proton and carbon atoms showed smaller displacements.

It is noteworthy that, unlike the amine protons, which are shielded upon coordination of DCF-en to platinum, the amidic proton resonates at lower fields in the complex. The ^{195}Pt-NMR spectrum of **1** in DMSO-d_6 (Supporting Information, Figure S2) showed one signal at –2,160 ppm, a chemical shift compatible with a Pt atom in a N_2Cl_2 coordination environment.[30]

The ESI-MS spectrum of complex **1** displays the molecular ion peak $[M + Cl]^-$ at 657.00. There is good agreement between the experimental isotopic pattern and the theoretical one (Supporting Information, Figure S3).

Using the same DCF-en ligand, a *trans*-platinum(II) compound was also synthesized (Scheme 3).

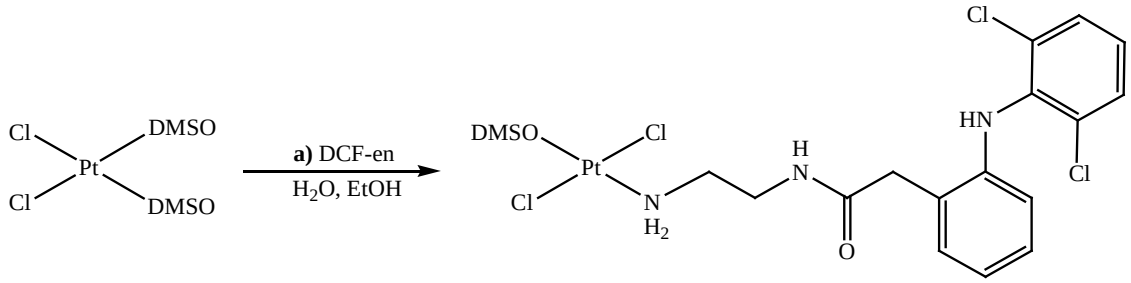

Scheme 3

Complex **2** was obtained by the addition of DCF-en to a solution of *cis*-$[PtCl_2(DMSO)_2]$ in water at 218 K. After 12 h reaction, addition of diethyl ether, afforded yellow crystals of *trans*-$[PtCl_2$(DCF-en)(DMSO)] in good yield. The obtainment of the *trans* isomer is in full agreement with literature data.[31]

The ^{1}H NMR spectrum of complex **2**, recorded in DMSO-d_6 (Supporting Information, Figure S4), was similar to that of compound **1** (Supporting Information, Table S1). In addition, the spectrum shows a singlet close to 3.34 ppm belonging to the methyl groups of the DMSO coordinated to platinum. Also in this case, the shift of the amine protons (3.65 ppm downfield) was indicative of NH_2 coordination. The coordination to the metal has also an effect on the chemical shifts of the proton and carbon atoms of the en-chain. The C3'H_2 protons undergo a little downfield shift (0.11 ppm), while the C2'H_2 protons undergo an upfield shifts (0.28 ppm). *C3'* presents a downfield shift of 3.9 ppm.

The ^{195}Pt NMR spectrum in DMSO-d_6 (Supporting Information, Figure S5) consists of a signal at –3,110 ppm. The chemical shift is in the range typical for a platinum(II) in a NCl_2S coordination environment.[30]

An ESI-MS spectrum of complex **2** was also recorded. The parent peak is present in the negative ions current at 680 m/z, corresponding to the species $[M - H]^-$. The fragmentation spectrum of the parent peak consists of two major signals falling at 602 and 566 *m/z*, corresponding to the species $[M - DMSO - H]^-$ and $[M - DMSO - HCl - H]^-$. There is good agreement between the experimental isotopic patterns and the theoretical one (Figure 6S).

X-ray Structure of 2. Crystals of **2** suitable for X-ray investigation were obtained from ethanol. Selected bond lengths and angles are given in Table 1. An ORTEP drawing of complex **2** is shown in Figure 4.

Table 1. Selected Bond Distances (Å) and Angles (°) for Complex 2.

Pt1—N1	2.069(9)	Pt1—Cl2	2.283(3)
Pt1—S4	2.211(3)	Pt1—Cl1	2.297(3)
N1—Pt1—S4	174.1(3)	N1—Pt1—Cl1	86.5(2)
N1—Pt1—Cl2	88.1(2)	S4—Pt1—Cl1	94.74(14)
S4—Pt1—Cl2	90.90(12)	Cl2—Pt1—Cl1	174.14(13)

The Pt atom has a roughly square planar coordination geometry and the donor atoms are two trans chlorines, one nitrogen, and one sulfur. The largest deviation from the plane defined by the four donor atoms concerns N1[0.20(1) Å].

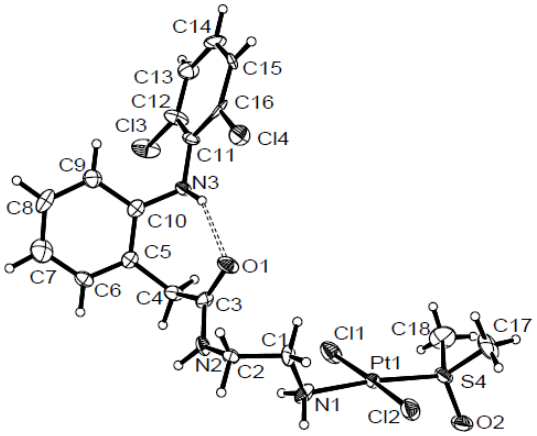

Figure 4. ORTEP view of *trans*-[$PtCl_2$(DCF-en)(DMSO)] **(2)** with the atom numbering scheme. Displacement ellipsoids are represented at 30% probability levels. An intramolecular hydrogen bond is shown in dashed line.

The platinum-ligand distances (2.069(9) Å for Pt-N, 2.211(3) Å for Pt-S, and 2.290(3) Å for mean Pt-Cl are in good agreement with values found in structurally related complexes.[32-34]

One intra-molecular hydrogen bond is present between the N–H group and the amidate oxygen of the DCF ligand [Figure 2, N3 ⋯O1 = 2.88(1) Å, N3—H⋯O1 = 146(3)°].

In the crystal packing, each molecule is linked to the adjacent molecules by three hydrogen bonds (one strong and two weak) (Supporting Information, Figure S7a and Table S2). In addition, there is a typical π···π stacking interaction between dichlorophenyl rings of two nearby molecules (dihedral angle of 0.01° with average distance of 3.86 Å and short contacts (3.532 Å) for C14–C16(-*x*-1,-*y*+2,-*z*+1) and C16–C14(-*x*-1,-*y*+2,-*z*+1) which are close to the sums of the van der Waals radii (Supporting Information, Figure S7b).[35]

Synthesis and Characterization of *cis*-[Pt(DCF)$_2$(NH$_3$)$_2$] (3). The *cis*-[Pt(DCF)$_2$(NH$_3$)$_2$] (**3**) complex was synthesized by direct reaction of *cis*-[Pt(NH$_3$)$_2$(H$_2$O)$_2$]$^{2+}$ with the sodium salt of DCF performed in water solution at 203 K (Scheme 4).

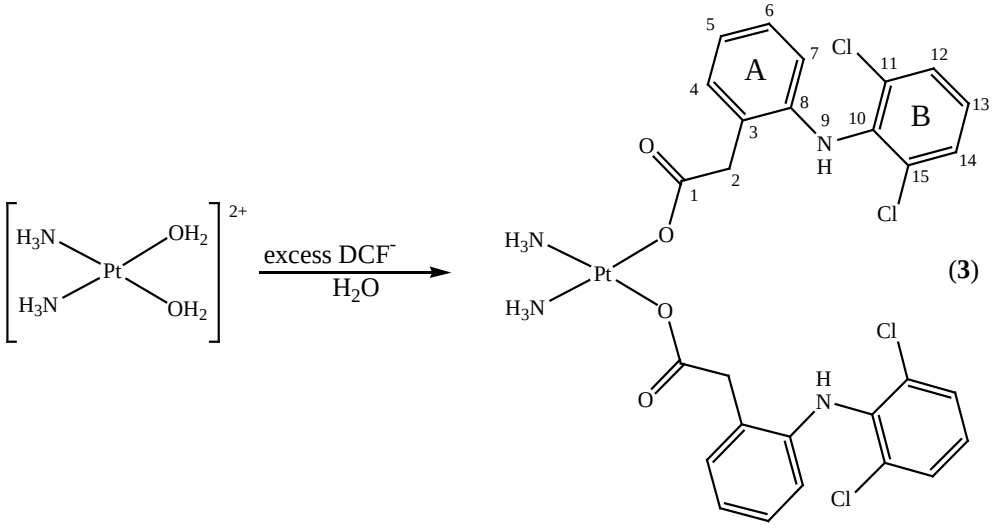

Scheme 4

The isolation of **3** was facilitated by its low solubility in water in which the starting materials are very soluble. The compound was obtained pure and in good yield, and was fully characterized by IR, multinuclear NMR spectroscopy, ESI-MS and elemental analysis. Spectroscopic and spectrometric features of the obtained compound were in accord with the proposed formulation.

All NMR signals could be unequivocally assigned on the basis of 1D and 2D correlation spectroscopy (COSY), heteronuclear multiple quantum correlation (HMQC) and heteronuclear multiple bond correlation (HMBC) experiments (Scheme 4 for the numbering of protons, Supporting Information, Table S1).

The ^{1}H-NMR spectrum of **3** in DMSO-*d*$_6$ (Supporting Information, Figure S8) shows DCF signals falling at 8.23 ppm for the aminic proton, five signals between 7.50 and 6.25 ppm for the aromatic protons, and one singlet at 3.50 ppm for the methylene protons. In addition, complex **3** shows a sharp signal close to 4.43 ppm belonging to the protons of the ammine ligands.

The five signals of the aromatic protons of DCF were assigned through 2D COSY and NOESY experiments (Supporting Information, Figures S8 and S9, respectively) recorded in DMSO-*d*$_6$.

The ^{1}H and ^{13}C chemical shift variations (with respect to the corresponding signals in the free ligand) (Δδ) were used to deduce the mode of coordination of DCF to the metal. The largest variations are always observed for the proton and carbon atoms located closer to the donor atom attached to the metal core.[36, 37] In complex **3** the largest shifts were observed for the methylene protons (3.47 ppm) which were shifted downfield by 0.10 ppm, and for C1 (which was shifted downfield by 4.3 ppm). All other proton and carbon signals suffered minor displacements with respect to the free ligand. Therefore, it is possible to conclude that DCF coordinates to platinum through the carboxylic group.

It is interesting to note that the aminic proton is less shielded in free DCF than in complex **3**. One plausible explanation is that in free DCF the aminic group forms an hydrogen bond with the carboxylic group;[38] this H bond is disrupted upon coordination of DCF to platinum.

The ^{195}Pt-NMR spectrum of complex **3** (Supporting Information, Figure S10) shows one signal at –1,563. This chemical shift lies within the range exhibited by platinum(II) complexes in a N_2O_2 coordination environment.[30]

The ESI-MS spectrum of **3** displays parent peak of high intensity corresponding to $[M + NO_3]^-$ at m/z 879.98. The MS/MS spectrum of the parent ion shows a major peak at m/z 643 corresponding to *[M – dic]*$^-$. There is good agreement between the isotopic pattern of the experimental peaks and the theoretical ones for complex **3** (Supporting Information, Figure S11).

Solvolysis of *cis*-[Pt(NH$_3$)$_2$(Dic)$_2$] (3) in DMSO and in a Mixture of DMSO and Water (4:1, v/v). Owing to the insolubility of **3** in aqueous solution, its solvolysis was investigated either in DMSO or in a mixture of DMSO and water (4:1, v/v) at 298 K. DMSO is widely used to dissolve insoluble drugs for biological experiments. The reaction progress was monitored by ^{1}H NMR spectra registered at different times. The signals corresponding to the starting compound decreased with time being replaced by two new sets of signals corresponding to the solvate species *cis*-$[Pt(NH_3)_2(Dic)(DMSO\text{-}d_6)]^+$ and to free DCF. The concentrations of different species were evaluated by integration of the signals belonging to the aminic proton of DCF falling in the range between 7.5 and 11 ppm. The kinetic data were in accord with a first order reaction and afforded a value for the rate constant of $1.0(\pm0.1)x10^{-4}$ s^{-1} corresponding to a $t_{1/2}$ of *ca.* 7000 s (Supporting Information, Figure S12). It can be noted that the hydrolysis of the second DCF ligand is much slower.

A second experiment was performed in which complex **3** was dissolved in a mixture of DMSO-d_6 and D_2O in the ratio of 4:1 v/v. The concentrations of different species were calculated by integration of the ^{1}H NMR signals belonging to the methylene protons of DCF falling in the range between 3.2 and 3.7 ppm. The kinetic data were in accord with a first order reaction and gave a rate constant of $7.0(\pm0.2)x10^{-5}$ s^{-1} corresponding to $t_{1/2}$ of *ca.* 9900 s. It can be concluded that the presence of water does not increase the rate of solvolysis with respect to pure DMSO. Also in this case the rate of solvolysis of the second DCF ligand is much slower.

A final experiment was performed in a mixture of DMSO-d_6/saline D_2O (9 mg NaCl in 1 mL of D_2O) in the ratio 4:1 v/v. As in the previous case, the concentration of different species was evaluated by integration of the signals belonging to the methylene protons of DCF falling in the range of 3.2-3.7 ppm in the ^{1}H NMR spectra. In this latter case other species are formed beyond *cis*-$[Pt(NH_3)_2(Dic)(DMSO\text{-}d_6)]^+$ and free DCF (as evidenced by the presence of additional signals in the region 3.2-3.7 ppm), possibly □hloride species. The estimated rate constant for the first order reaction is $4.0(\pm0.2)x10^{-5}$ s^{-1}. This value is only slightly smaller than that found in the experiment performed in pure DMSO/water. In this case the solvolysis of the second DCF ligand is significantly faster with respect to the previous two cases.

Overall, the rate constants for first solvolysis of DCF ligand fall in the range of 4-10 $x10^{-5}$ s^{-1}. These values are only slightly bigger than that reported for cisplatin in water at 298 K ($1.9x10^{-5}$ s^{-1}),[39] but significantly bigger than those reported for *trans*-$[Pt(OOCCH_3)_2(NH_3)L]$ complexes (L = 2-, 3- or 4-picoline), always in water but at 310 K, which were in the range 1-$4x10^{-6}$ s^{-1}.[40, 41] A slow rate of solvolysis of the trans-acetato complexes is expected on the basis of the low trans effect of O-donor with respect to N-donor ligands. Instead, a quite higher rate of solvolysis ($7.1x10^{-4}$ s^{-1} at 298 K) has been reported for the *cis*-$[Pt(OOCCH_3)_2(dbtp)_2]$ complex (dbtp=5,7–diterbutyl-1,2,4-triazolo[1,5-a]pyrimidine).[42] The one-order of magnitude difference with respect to our values can be accounted for on the bases of different trans effect of trans ligands (N-donor aromatic base with respect to ammine) and, in part, to the different solvent.

Cytotoxicity. The cytotoxic activities of **1-3** were determined against cisplatin sensitive A2780 and cisplatin resistant A2780cisR human ovarian carcinoma cell lines, commonly used to test cytotoxic activity of cisplatin derivatives and other platinum-based drugs. Moreover, two COX-2 positive cell lines (HT-29 and HeLa) were also included because DCF is a well-known inhibitor of COX-2. This cyclooxygenase is a rate limiting enzyme in the synthesis of prostaglandins, which is mainly produced in response to tissue damages and pro-inflammatory signals.[43, 44] Notably, COX

overexpression can promote carcinogenesis, invasion, and metastasis processes as well as tumor angiogenesis.[44]

The tumor cell lines were incubated with the platinum compounds or free DCF for 72 h and cell survival in cultures was evaluated as described in detail in Experimental section. The IC_{50} values (concentration of compound which causes death in 50% of cells) are reported in Table 2.

Table 2. Cytotoxicity (IC_{50} mean values[a], μM).

	A2780	A2780cisR	RF[b]	SW480	HeLa	HT-29	MRC-5 pd30
1	8.5 ± 0.8	14.1 ± 0.7	1.66	10.66 ± 0.03	16.9 ± 0.4	11.6 ± 0.5	15.8 ± 0.5
2	31.3 ± 2.2	23.4 ± 1.2	0.75	17.3 ± 0.7	17.1 ± 0.7	14.0 ± 0.4	19.9 ± 0.5
3	1.61 ± 0.03	3.16 ± 0.03	1.96	2.8 ± 0.2	3.6 ± 0.1	4.4 ± 0.1	6.61 ± 0.09
cisplatin	3.1 ± 0.1	16.7 ± 2.2	5.39	2.6 ± 0.2	22.8 ± 0.9	13.3 ± 0.5	3.07 ± 0.03
DCF	238 ± 19	138 ± 8	0.58	254 ± 29	238 ± 6	184 ± 5	451 ± 28

[a]The results are expressed as mean values ± SD of three independent experiments, each made in triplicate

[b]RF – Resistance factor, defined as IC_{50} (resistant, A2780cisR)/IC_{50} (sensitive, A2780).

All tree Pt(II)-DCF conjugates tested in this work showed promising cytotoxic activity. In COX-2 deficient cell lines (A2780, A2780cisR and SW480), the cis compounds **1** and **3** were significantly more effective compared to the trans-complex **2**, being comparable to (**1**) or even more effective (**3**) than clinically used cisplatin. Importantly, the resistance factor was significantly lower in the case of DCF-containing complexes compared to that of cisplatin. This suggests that the mechanism underlying the biological action of these complexes is at least partially different from that of cisplatin, allowing the compounds to overcome successfully the resistance mechanisms acting in the case of cisplatin.

Apart from the ability of **3** to affect tumor cells resistant to clinically used cisplatin, the low cytotoxicity of **3** in noncancerous human cells derived from normal lung tissue (Table 1) demands special attention. The IC_{50} values of **3** in noncancerous cells (MRC-5 pd30) are more than 4-fold greater than that found for the sensitive cancer cell line A2780. Thus, **3**, in contrast to cisplatin, shows selectivity towards tumor cells relative to nontumorigenic normal cells (Table 1). Hence, these data show that in contrast to free cisplatin, **3** may be recognized as a promising approach to improving the therapeutic index of platinum anticancer agents.

Interestingly, unlike the case of COX-2 negative cells, there was no significant difference between the cytotoxic effectivities of cis- and trans-complexes **1** and **2** in the case of COX-2 positive cancer cell lines HeLa and HT-29. This may suggest that the COX-2 inhibitory effect of the DCF ligand can play a role in the COX-2 positive cells and it is independent from the complex configuration.

Although COX is the only molecular target hitherto recognized for the anti-inflammatory activity of DCF (and other NSAIDs), both COX dependent and COX-independent mechanisms in the mode of anticancer action of NSAIDs have been reported.[45-47] It was previously demonstrated that DCF targets glucose metabolism and proliferation in tumor cells by inhibiting both the transcription factor MYC and the lactate transporters,[19] leading to blockage of the glycolytic process and reverting the Wartburg effect. In addition, DCF is known to stimulate basal and uncoupled respiration, inhibits ATP synthesis, and collapses membrane potential in mitochondria.[20] Therefore, the next experiments were aimed at probing the biological manifestation of DCF ligand(s) in the Pt(II) derivatives tested in the present work. We have investigated the potential factors involved in the mechanism underlying the cytotoxic effects for a representative of this group of compounds, that which exhibited the highest toxicity in tumor cell lines (Table 2), namely

compound **3**. We compared these factors to those involved in the mechanism underlying the cytotoxic effects of the parent metallodrug cisplatin and free DCF.

DCF Ligands in *cis*-[Pt(DCF)$_2$(NH$_3$)$_2$] (3) Enhance Cellular Accumulation of Platinum. The cellular accumulation of platinum from **3** and cisplatin in the human ovarian carcinoma cell lines A2780 (cisplatin-sensitive), its variant (A2780cisR) with acquired resistance to cisplatin,[48, 49] and the human cervical carcinoma HeLa cells was investigated for possible relationship between the cellular uptake and *in vitro* cytotoxicity of **3**. Cellular concentrations of platinum from **3** or cisplatin were determined by flameless atomic absorption spectrometry (FAAS) after 24 h of exposure to the complexes at the concentration of 10 μM. The results are summarized in Table 3.

Table 3. Cellular Uptake of Platinum from Cisplatin and 3 (pmole Pt/10^6 cells) into A2780, A2780cisR, and HeLa Cells after 24 h of Drug Exposure (10 μM).

	A2780	A2780cisR	HeLa	log P[#]
Cisplatin	96 ± 3	31 ± 2	110 ± 10	-2.26 ± 0.02
3	370 ± 20	250 ± 10	1410 ± 10	0.65 ± 0.07
DCF	ND	ND	ND	1.12 ± 0.03

[#] Log P (octanol/water) values measured by "shake flask" method at room temperature. All results are expressed as mean values ± SD from at least three independent experiments.

The replacement of cisplatin chlorides by DCF resulted in a significant enhancement of the cellular platinum uptake. To quantify the hydrophobicity of the platinum complexes, partition coefficients (log P) values for octanol/water partition were measured using the shake-flask method. The log P values for **3**, cisplatin, and free DCF are also shown in Table 3. Cisplatin is hydrophilic (partition preferentially into water) while **3** is hydrophobic (partition preferentially into octanol). The results of cellular accumulation of platinum from **3** and cisplatin are consistent with the premise that hydrophobic rather than hydrophilic platinum compounds penetrate more easily the cytoplasmic membrane, which leads to their increased cellular accumulation.

Notably, the ratio of the cell associated Pt levels of A2780/A2780cisR is markedly higher for cisplatin than for its derivative **3** (~2.1-fold) suggesting that facilitated transport, possibly involving copper transporters,[50] increases the cellular accumulation of cisplatin in the sensitive A2780 cells much more than in the resistant A2780cisR cells resulting in the higher values of resistance factor (RF) for cisplatin compared with **3** (2.0 vs. 5.4, Table 3). Thus, it is reasonable to suggest that the presence of DCF in **3** enhances the hydrophobicity, thereby significantly facilitating association of this conjugate with cells and enhancing its cytotoxicity. This also suggests that the different mechanism of cellular uptake in comparison with cisplatin contributes to the ability of **3,** containing DCF ligands, to overcome resistance of tumor cells to cisplatin.

DNA-bound Platinum in Cells Exposed to *cis*-[Pt(DCF)$_2$(NH$_3$)$_2$] (3). DNA is believed to be the target for antitumor cisplatin and its direct derivatives. For this reason, DNA from HeLa cells after exposure to 10 μM cisplatin or **3** for 2, 5, 10 and 24 h was isolated and the levels of platinum on DNA were determined by inductively coupled plasma mass spectroscopy (ICP-MS) (Figure 5). The platinum content of DNA from the HeLa cells treated with **3** was markedly higher (approximately 7-8-fold greater for 10 or 24 h incubation) than that from the cells treated with cisplatin. Thus, DNA-bound platinum in HeLa cells exposed to **3** parallels the results of cell accumulation of this platinum complex and is consistent with the view and supports the hypothesis that **3** after its accumulation in the cells is aquated and thereby also releases DCF molecules enabling a dual action mode (that of cisplatin and that of DCF).

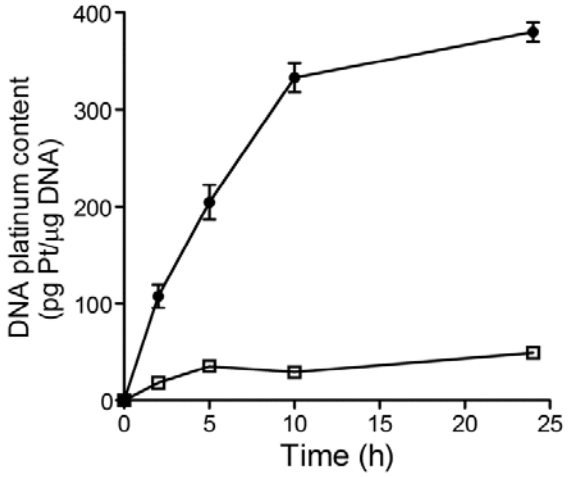

Figure 5. Time dependence of platinum content of DNA isolated from HeLa cells treated with **3** (●) or cisplatin (□) at 10 μM concentration for 2 - 24 h. The data represent mean values ± standard deviations from at least three independent experiments. For other details, see the text.

The observation that DNA from the cells treated with **3** is effectively platinated **(**Figure 5) deserves a further discussion. A compound closely related to **3** is carboplatin containing the bidentate dicarboxylate leaving ligand which is a poorer leaving group than chlorides in cisplatin. Hence, carboplatin in the absence of acid and nucleophiles is stable in water and platinates in such a medium DNA markedly less than cisplatin. Similarly to carboplatin, the DCF ligands in **3** [coordinated to Pt(II) via their carboxylic group] can be expected to be poor leaving groups. The fact that carboplatin effectively platinates DNA in treated cells has been explained by its activation by nucleophiles and the more acidic pH in tumor cells favoring the removal of the malonate and formation of acquated cisplatin. It is therefore reasonable to assume also for **3** that, after accumulation of intact **3** in cells, it undergoes activation in a similar way resulting in removal of the parental molecules of DCF. Hence, the effective platination of DNA from the cells treated with **3** is consistent with the view and supports the hypothesis that after **3** accumulates in tumor cells treated by this conjugate at low micromolar concentrations, parental DCF molecules are released in a significant amount necessary for manifestation of their biological functions. Notably, various prodrugs derived from NSAIDs containing carboxylic group were prepared in which the carboxylic group was masked, but it has been shown that a major requisite for these prodrugs is that they must be readily hydrolyzed, enzymatically or chemically, to quantitatively release the parent NSAID drug.[51]

DCF Ligands Released from *cis*-[Pt(DCF)$_2$(NH$_3$)$_2$] (3) Alter Cell Cycle Profile. To further characterize the cytotoxic effect of **3**, an analysis of the cell cycle perturbations was performed in HeLa cells exposed to **3**, or to the reference compound cisplatin and free DCF. Activation of cell cycle checkpoints is a general cellular response to cytotoxic agents. Cells were exposed to **3**, cisplatin or free DCF at their equitoxic concentrations for 24 h. Significant differences in cell cycle modulation between **3** and cisplatin were observed (Table 4 and Supporting Information, Figure S13). Cells treated with cisplatin were blocked mostly at S phase of the cell cycle and were depleted of G_2/M-phase cells. This observation is in agreement with the previously reported data.[52] The cell cycle distribution profile of HeLa cells treated with **3** differed from that of cells treated with cisplatin in two aspects. First, the S phase fraction was decreased while the G_2/M phase fraction significantly increased suggesting the potentiation of the effect of cisplatin by DCF. Second, increased amount of sub-G_1 phase material was present indicating that a greater fraction of the cells has undergone disintegration and possibly apoptosis. Besides, cells treated with free DCF were

considerably blocked at the S and G_2/M phases of cell cycle when compared to the untreated (control) cells. Taken together, these results suggest that DCF ligands affect distribution of cells in individual phases of the cell cycle in comparison with the effects of cisplatin and permit the damaged cells to traverse the S phase. The data showed that treatment of the HeLa cells with **3** altered their cell cycle profile in a way different from that of parental cisplatin. These data are also consistent with the hypothesis that DCF ligands play an important role in enhanced antiproliferative activity of the new class of Pt(II) complexes containing DCF ligands.

Table 4. Cell-cycle Distribution of HeLa Cells after 24-h Treatment with Cisplatin, 3 and Free DCF.[a]

	subG1	G1	S	G2
Control	1.2 ± 0.3	78 ± 2	11 ± 1	8.0 ± 0.9
Cisplatin	$2.5 \pm 0.1^{\star,\S}$	$60 \pm 2^{\star,\S}$	$38 \pm 1^{\star,\S}$	$0.1 \pm 0.1^{\star,\S}$
3	$9.2 \pm 1.9^{\star,\#,\S}$	$63 \pm 2^{\star,\S}$	$22 \pm 2^{\star,\#,\S}$	$6.1 \pm 0.3^{\#,\S}$
DCF	$5.6 \pm 1.4^{\star,\#}$	$52 \pm 1^{\star,\#}$	$29 \pm 2^{\star,\#}$	$13 \pm 1^{\star,\#}$

[a]Effects of cisplatin, **3** and free DCF on cell cycle distribution of HeLa cells. Untreated (control) cells or cells treated for 24 h with roughly equitoxic concentrations (three-fold values of IC_{50} found for these compounds in HeLa cells treated for 72 h, Table 2) were harvested, fixed, stained with propidium iodide, and assessed for cell cycle distribution by FACS analysis. The estimated percentages of HeLa cells in different phases of the cell cycle were acquired using ModFit software and are expressed as the mean ± SD of three independent experiments. The symbols ★, # and § denote significant difference ($p < 0.05$) from the untreated control, cells treated with cisplatin and free DCF, respectively.

***Cis*-[Pt(DCF)$_2$(NH$_3$)$_2$] (3) Targets Glucose Metabolism in Tumor Cells.** It was demonstrated previously that DCF, in contrast to other NSAIDs, targets tumor cell glucose metabolism by causing the decrease of lactate secretion,[19] leading to blockage of the glycolytic process and reverting the Wartburg effect. Interestingly, a recent report indicates that increased lactate concentrations in the tumor correlate with malignancy[53] and the escape of some malignant tumors from immune surveillance.[54, 55]

In this study we hypothesized that upon intracellular hydrolysis of **3**, besides the platinum moiety able to interact with its key target nuclear DNA, free DFC molecules would be also released, which could promote apoptosis also through inhibition of lactate transporters resulting in blockage of the glycolytic process.[19] We determined lactate in the supernatant of A2780 and A2780cisR cells treated with **3** and for comparative purposes with cisplatin and free DCF for 6 h. After this period, cells were removed by centrifugation and lactate concentration in cell culture medium was measured using a colorimetric Lactate Assay Kit (Sigma-Aldrich). In this assay, lactate concentration is determined by an enzymatic assay, which results in a colorimetric (570 nm) product proportional to the lactate present in the medium. The results are shown in Figure 6A and reveal that treatment of ovarian cancer cells with **3** resulted in a significant decrease of the level of extracellular lactate, similarly to the effect of free DCF. In contrast, treatment with cisplatin resulted in no significant changes in the level of extracellular lactate. Thus, in the case of **3** an inhibition of glycolysis and/or lactate transport (not observed for cisplatin) can be attributed to the DCF ligands present in this conjugate and released upon intracellular hydrolysis.

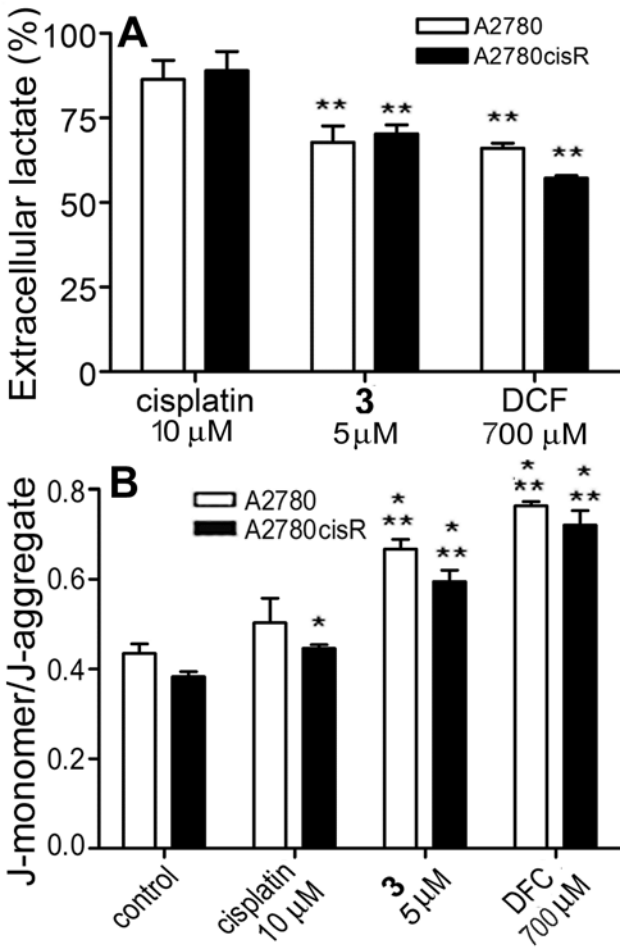

Figure 6. A. Modulation of extracellular lactate level in A2780 and A2780cisR cells after 6-h treatment with cisplatin, **3**, or free DCF at the concentrations indicated in the graph (these concentrations correspond approximately to three-fold values of IC_{50} found for these compounds in A2780 cells treated for 72 h). The amount of lactate produced was measured in cell culture medium by an enzymatic colorimetric assay. The level of lactate in the medium containing untreated control cells was taken as 100%.
B. Changes in the mitochondrial membrane potential $\Delta\psi_m$ in A2780 and A2780cisR cells. Cells were treated for 6 h cisplatin, **3**, or free DCF at the concentrations indicated in the graph [these concentrations correspond approximately to three-fold values of IC_{50} found for these compounds in A2780 cells treated for 72 h, (Table 2)], cells were subsequently stained with JC-1 and fluorescence was determined by confocal microscopy (for other details, see the text). Results represent mean ± SD from three independent experiments. The symbols (★,★★) denote a significant difference ($p<0.05$) from the untreated control and the cells treated with cisplatin, respectively.

***Cis*-[Pt(DCF)$_2$(NH$_3$)$_2$] (3) Affects Mitochondrial Transmembrane Potential in Tumor Cells.** DCF has shown novel COX-independent antitumor effects caused by its influencing mitochondrial activity[19] Moreover, it was observed that DFC stimulates basal and uncoupled respiration, inhibits ATP synthesis, and collapses membrane potential in mitochondria.[20] The reduction of mitochondrial activity might contribute to the anti-proliferative effect of DFC on tumor cells.

To provide evidence whether the DFC, delivered to cancer cells by the Pt(II) complex bearing this potential metabolic modulator, promotes cell death by a mitochondrial-regulated mechanism, we determined changes in the mitochondrial transmembrane potential ($\Delta\psi_m$) in A2780 and A2780cisR cells induced by **3**. We used a cationic dye JC-1 (5,5′,6,6′-tetrachloro-1,1′,3,3′-tetraethylbenzimidazolylcarbocyanine iodide) that exhibits potential-dependent accumulation in the

mitochondria accompanied by a shift of fluorescence emission due to the concentration-dependent formation of green fluorescent 'J-monomers' and red fluorescent 'J-aggregates'. Mitochondrial depolarization is indicated by an increase in the green/red fluorescence intensity ratio. The effect of **3**, cisplatin and free DCF on the $\Delta\psi_m$ in A2780 and A2780cisR cells after 6-h treatment is represented in Figure 6B and in the Supporting Information, Figure S14. Quantitative analysis of JC-1-stained tumor cells revealed a slight increase in the green (low $\Delta\Psi_m$) to red (high $\Delta\psi_m$) fluorescence ratio in cisplatin treated A2780 cells (0.50 ± 0.06) and A2780cisR cells (0.45 ± 0.01) compared to untreated control cells (0.44 ± 0.02 and 0.38 ± 0.01). Notably, **3** displayed significant mitochondrial depolarization in both cell lines (0.67 ± 0.02 and 0.60 ± 0.03) compared to control and even markedly higher than those for cisplatin. As a positive control of $\Delta\psi_m$ depolarization, was used free DCF at the equitoxic concentration (which was approximately 2 orders of magnitude higher than that of the platinum complexes). The data in Figure 6B and in the Supporting Information, Figure S14 demonstrate an expected marked mitochondrial depolarization in both cell lines tested (0.76 ± 0.01 and 0.72 ± 0.03) compared to untreated control and cisplatin treated cells.

The results of these experiments indicate the ability of **3** to collapse mitochondrial membrane potential ($\Delta\psi_m$) in A2780 and A2780cisR human ovarian cancer cells due to the presence of metabolically active DFC ligands. In other words, reduction of $\Delta\psi_m$ caused by concentrations of **3** which were approximately two orders of magnitude lower than those of free DCF, can be attributed to the DCF molecules released upon hydrolysis of **3** inside tumor cells. Thus, these data establish mitochondria as one of the major mediators of the antiproliferative effect of Pt(II)-DCF conjugates in cancer cell lines.

***Cis*-[Pt(DCF)$_2$(NH3)2] (3) Decreases Invasion, Migration and Re-adhesion of Tumor Cells.** In addition to the anticancer effect attributed to the COX-independent effects on mitochondrial activity, DCF has also shown effects caused by the inhibition of COX-1 and COX-2 enzymes. In general, NSAIDs are routinely used to treat a wide variety of pathologies. Their anti-inflammatory activity is due to the inhibition of the COX system that catalyzes conversion of arachidonic acid to prostaglandins, which are the mediators of the inflammatory process.[2, 3] COX-1 is a constitutive isoform which is present in the majority of normal cells and tissues, while the inducible isoform COX-2 is highly expressed in aggressive metastatic cancers and may play a critical role in cancer progression (i.e. growth and metastasis). Therefore, we also investigated the antimetastatic activity of the Pt(II) conjugate **3,** containing two DCF ligands, which has shown extensive antiproliferative effect in COX-2 expressing HT-29 and HeLa cells (Table 3). An initial step in tumor metastasis is invasion of cancer cells into surrounding tissue and the vasculature which requires chemotactic migration of cancer cells.[56] In addition, invasive and migratory properties of tumor cells are closely connected with their adhesivity.[57] Therefore, we evaluated in the present work the invasion, migration and re-adhesion activities of these cells treated with cisplatin, **3** and free DCF as a measure of their metastatic potential.

The effects on invasion activity was assessed using a matrigel transwell assay as described in Experimental section. The treatment of tumor cells for 1 h with **3** resulted in a significantly reduced invasion activity, in particular when the cells were treated with equimolar concentrations of the agents (Figures 7A,B). This reduced effect was more apparent than that observed for the cells treated with free DCF except in the case of HT-29 cells when treated with **3** and free DCF at equitoxic concentrations. Interestingly, the treatment with cisplatin also resulted in a decrease in invasion ability of the cells in agreement with previously published results,[58, 59] although this effect was only slightly less pronounced than that observed for **3**. When the cells were treated with these agents at equimolar concentrations. These results suggest that presence of DCF ligands in **3** contributes to its efficiency to reduce invasion activity of tumor cells expressing COX-2.

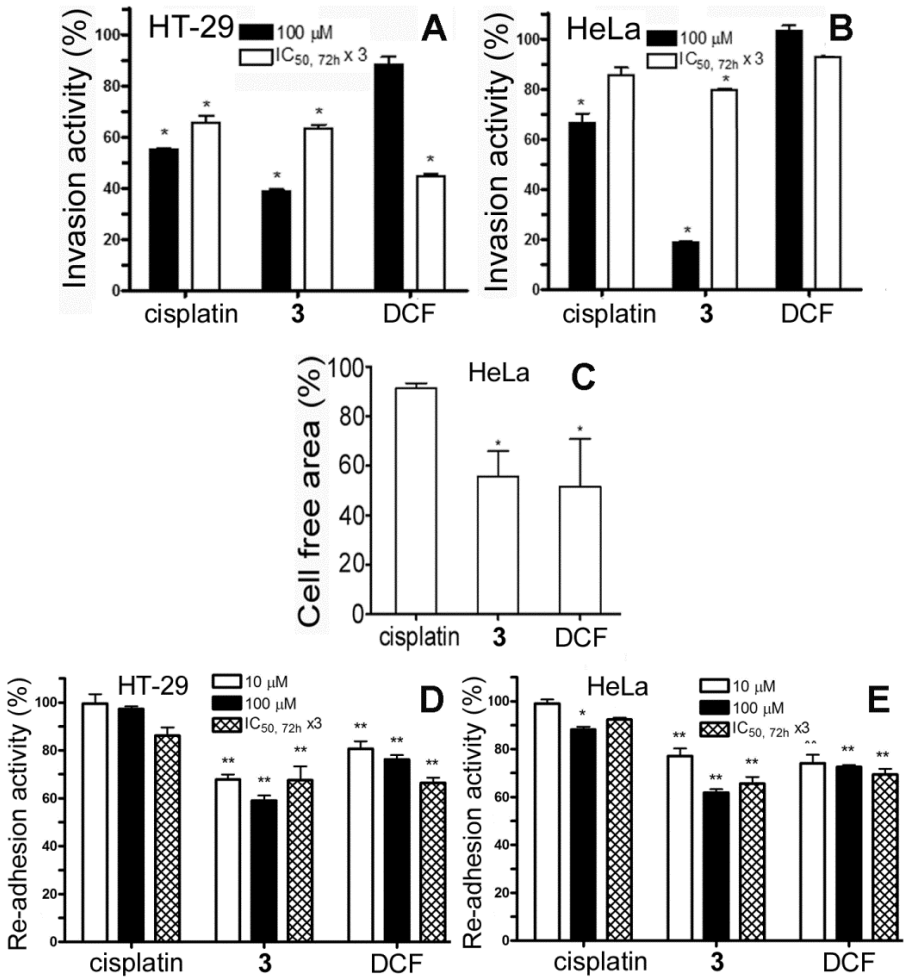

Figure 7. Effect of **3**, cisplatin and free DCF on invasion, migration and re-adhesion activity of HT-29 and HeLa cells.

A,B. HT-29 or HeLa cells were treated for 1 h with equimolar (100 μM) or roughly equitoxic concentrations of cisplatin, **3**, or free DCF [these concentrations correspond approximately to three-fold values of IC_{50} found for these compounds in HT-29 or HeLa cells treated for 72 h ($IC_{50,72h}$, Table 2)]. Cell invasion activity was measured as described in the Experimental section and is expressed relative to the untreated control. Time for invasion was 96 h. Stars at the top of the bars denote significant difference ($p < 0.05$) from control $p < 0.05$. Experiments were performed in triplicate.

C. The cell-free area 24 h after addition of cisplatin, **3** or free DCF was measured at their roughly equitoxic concentrations [15, 2.3, or 150 μM, respectively; these concentrations correspond approximately to 0.65 % values of IC_{50} found for these compounds in HeLa cells treated for 72 h (Table 2)] when a wound was also made as described in the Experimental section and is expressed relative to the control. Stars (★) at the top of the bars denote significant difference ($p < 0.05$) from control. Experiments were performed in triplicate.

D,E. HT-29 or HeLa cells were treated for 1 h with cisplatin, **3** or free DCF at equimolar (10 or 100 μM) or roughly equitoxic concentrations of cisplatin, **3**, or free DCF [these concentrations correspond approximately to three-fold values of IC_{50} found for these compounds in HT-29 or HeLa cells treated for 72 h ($IC_{50,72h}$ x 3, Table 2)]. The time for the reconstitution of membrane adhesive proteins after the detachment was 30 min followed by 30 min incubation at 236 K for the cellular re-adhesion. Cell re-adhesion activity was measured as described in the Experimental section and is expressed relative to the untreated control. The star (★) at the top of the bar denotes significant difference from the untreated control, $p < 0.05$; two stars (★★) at the top of the bars denote

significant difference from both untreated control and cells treated with cisplatin, $p < 0.05$. Experiments were performed in triplicate with octuplicate runs of each sample.

Malignant cancer cells utilize their intrinsic migratory ability to invade adjacent tissues and the vasculature, and ultimately to metastasize.[60] The results in Figures 7A,B suggest that when HT-29 or HeLa cells are treated with **3** their migration activity is diminished and that the enhanced inhibition of the cell migration is due to the presence of DCF ligands in **3**. We tested this hypothesis by evaluating the anti-migratory effects of cisplatin, **3** and free DCF in wound healing assays using the HeLa cell line; we measured the cell-free area 24 h after addition of cisplatin, **3** and free DCF at their equitoxic concentrations to the cells when a wound was also made. Under these experimental conditions, the higher cell-free area means the lower cell migration activity. As shown in Figure 7C and the Supporting Information, Figure S15, **3** reduced the ability of HeLa cells to close artificial wounds, i.e., scratches, in monolayers when compared to untreated control cells (100% wound healing). The potency of free DCF at the equitoxic concentration to inhibit cell migration was similar whereas that of cisplatin was markedly less. Thus, the results of these experiments show that the presence of DCF ligands in **3** contributes to the inhibition of invasion and migration activity of cancer cells.

The evaluation of the effects of **3** on its pharmacological properties was also tested on the capacity of this agent to inhibit the adhesion properties of HT-29 and HeLa cells *in vitro*. We used the test described previously[61] which made it possible to study the effect of **3**, cisplatin and free DCF on the ability of HT-29 and HeLa cells to re-adhere to a growth surface (Figures 7D,E).

Cisplatin affected the re-adhesion of HT-29 and HeLa cells to their plastic substrate of growth only negligibly. In contrast, **3** significantly reduced the re-adhesion of the treated cells even more than free DCA (Figures 7D,E).

In summary, the presence of DCF ligands in the molecule of **3** can effectively contribute to the ability of this Pt(II)-NSAID conjugate to suppress the cellular properties characteristic for metastatic progression, such as invasiveness, migration and re-adherence to a substrate.

CONCLUSIONS

Our study demonstrates that Pt(II) derivatives of cisplatin containing DCF ligand(s) with various intracellularly cleavable linkers are potent cytotoxic agents against several different cancer cell lines; they are also significantly more potent than cisplatin in a cisplatin-resistant tumor cell line. Interestingly, compound **3**, in which DCF molecules are coordinated to Pt(II) through their carboxylic group, is markedly more potent than its congeners (compounds **1** and **2** in which DCF ligands are conjugated to Pt(II) via a diamine) and cisplatin in COX-2 positive cell lines. These results indicate that the DCF ligand can play a role in the COX-2 positive cells in contrast to the conjugates of cisplatin with other NSAIDs, executing their cytotoxic action via COX-independent mechanisms. The replacement of cisplatin chlorides by DCF in compound **3** results in a significant enhancement of the cellular platinum uptake and concomitant markedly enhanced DNA binding. Thus, DNA-bound platinum in tumor cells exposed to **3** is consistent with the view and supports the hypothesis that **3** after its accumulation in the cells is aquated and thereby also releases DCF molecules enabling a dual action mode (that of cisplatin and that of DCF). Once inside the cell, DCF ligands released upon intracellular hydrolysis potentiate cisplatin moiety in **3** to induce cell cycle arrest, permit the damaged cells to traverse the S phase, inhibit glycolysis and/or lactate transport (not observed for cisplatin) and collapse mitochondrial membrane potential. Although designed to enhance antiproliferative activity, the presence of DCF ligands in the molecule of **3** can effectively contribute to the ability of this Pt(II)-NSAID conjugate to suppress the cellular properties characteristic for metastatic progression, such as invasiveness, migration and re-

adherence to a substrate. In aggregate, in this paper we show that the concept based on conjugations of platinum(II) complexes with the potent NSAID, such as DCF, can lead to "multi-functional" agents acting on different mechanistic levels. These agents, after they get into the cells, can trigger a number of processes that lead to both cytotoxic and anti-metastatic effects.

EXPERIMENTAL SECTION

Materials and Methods. Commercial reagent grade chemicals and solvents were used as received without further purification. *Cis*-[$PtI_2(NH_3)_2$],[62] K[$PtCl_3(NH_3)$],[63] and *cis*-[$PtCl_2(DMSO)_2$][64] were prepared according to already reported procedures. The elemental analysis and the spectroscopic features were fully consistent with the data reported in the literature.

Physical Measurements. NMR spectra were collected at 251 K on a Bruker AVANCE DPX 300 MHz nominal ^{1}H Larmor frequency. ^{1}H chemical shifts were referenced to TMS by using the residual protic peak of the solvent (DMSO-d_6) as internal reference. One-dimensional ^{195}Pt spectra were acquired using ^{1}H decoupling sequences. ^{195}Pt chemical shifts were referenced to K_2PtCl_4 (1 M in water, $\delta = -1{,}614$ ppm). Elemental analyses were carried out on a CHN Eurovector EA 3011 equipment. ESI-MS analyses were performed on an Agilent 1100 series LC-MSD Trap system VL. The analyses with the aid of ICP-MS or FAAS were performed using an Agilent 7500 instrument (Agilent, Japan) or Varian AA240Z Zeeman atomic absorption spectrometer equipped with a GTA 120 graphite tube atomizer.

Synthesis. *Preparation of 2-Aminoethyl diclofenacamide (DCF-en) ligand*. DCF-en was prepared from DCF and ethylenediamine. A suspension of DCF (0.914 g, 3.08 mmol) in $CHCl_3$ (13 mL) was treated with a three-fold excess of carbonyldiimidazole (1.502 g, 9.26 mmol). The reaction mixture was stirred for 5 min at room temperature and then extracted several times with water. The organic layer was dried over sodium sulfate and filtered. The solution was treated with ethylenediamine (0.741 g, 12.34 mmol), the reaction mixture was stirred for 10 min at room temperature and then extracted several times with water. The organic layer was dried over sodium sulfate, filtered and evaporated under reduced pressure. The crude residue was dissolved in HCl (3 M) and the solution filtered to remove insoluble impurities. After neutralization with KOH, the white solid was recovered by filtration of the mother solution and left to dry under vacuum. Obtained 0.550 g (1.63 mmol, 53% yield) of DCF-en. Anal. Calculated for DCF-en·H_2O ($C_{16}H_{17}N_3Cl_2O\cdot H_2O$): C, 53.94; H, 5.38; N, 11.80%. Found C, 53.49; H, 5.07; N, 11.42%. ^{1}H- and ^{13}C-NMR (DMSO-d_6) data are reported in Table 1S. ESI-MS: calculated for $[M + Na]^+$ $[C_{16}H_{17}N_3Cl_2Ona]^+$ 360.06. Found: *m/z* (% relative to the base peak) 360.10 (100).

*Preparation of cis-[$PtCl_2$(DCF-en)(NH_3)] (**1**).* K[$PtCl_3(NH_3)$] (0.200 g, 0.56 mmol) and tetraphenylphosphonium chloride (0.220 g, 0.56 mmol) were dissolved in CH_2Cl_2, then DCF-en (0.190 g, 0.56 mmol) was added and the reaction mixture stirred for 12 h at room temperature, meanwhile a pale yellow precipitate formed. The solid was collected by filtration of the mother solution, washed with CH_2Cl_2, and dried under vacuum. Obtained 0.120 g (0.20 mmol, 36% yield) of *cis*-[$PtCl_2$(DCF-en)(NH_3)] (**1**). Anal. Calculated for *cis*-[$PtCl_2$(DCF-en)(NH_3)] ($C_{16}H_{20}N_4Ocl_4Pt\cdot 3/2H_2O$): C, 29.61; H, 3.55; N, 8.63%. Found: C, 29.07; H, 3.29; N, 8.75%. ^{1}H- and ^{13}C-NMR (DMSO-d_6) data are reported in Table 1S. ^{195}Pt-NMR (DMSO-d_6) δ: –2,160 ppm. ESI-MS: calculated for $[M + Cl]^-$, $[C_{16}H_{20}N_4Ocl_5Pt]^-$, 656.97 Found*: m/z* (% relative to the base peak) 657.00 (100).

*Preparation of trans-[$PtCl_2$(DCF-en)(DMSO)] (**2**).* A solution of *cis*-[$PtCl_2(DMSO)_2$] (0.100 g, 0.23 mmol) in water (30 mL) was treated with a stoichiometric amount of DCF-en (0.080 g, 0.23 mmol). The reaction mixture was stirred at 203 K for 20 min and then treated with 50 mL of absolute ethanol and the solvent evaporated under vacuum. The white residue was treated with ethanol and kept under stirring at 218 K for 12 h; then the suspension was filtered. The mother liquor, concentrated to a minimum volume under reduced pressure, while keeping the reaction

vessel at 218 K, was treated with diethyl ether and then cooled to 269 K in order to induce precipitation of the desired product. Pale yellow crystals of **2** were deposited after a few days. The crystals were transferred on a glass filter, washed with diethyl ether and dried under vacuum. Obtained 0.090 g (0.13 mmol, 57% yield) of *trans*-[$PtCl_2$(DCF-en)(DMSO)] (**2**). Anal. Calculated for *trans*-[$PtCl_2$(DCF-en)(DMSO)] ($C_{18}H_{23}N_3O_2Cl_4SPt$): C, 31.69; H, 3.37; N, 6.16%. Found: C, 31.68; H, 3.58; N, 5.91%.^{1}H- and ^{13}C-NMR (DMSO-d_6) data are reported in Table 1S. ^{195}Pt-NMR (DMSO-d_6) δ: –3,110 ppm. ESI-MS: calculated for $[M - H]^-$, $[C_{18}H_{22}N_3O_2Cl_4SPt]^-$, 679.98. Found*: m/z* (% relative to the base peak) 680.00 (100).

Preparation of cis-[$Pt(DCF)_2(NH_3)_2$] (**3**). C*is*-[$PtI_2(NH_3)_2$] (0.250 g, 0.52 mmol) was suspended in water (20 mL) and treated with a 2-fold excess of $AgNO_3$ (0.1766 g, 1.04 mmol) previously solubilized in water (1 mL). The mixture was kept under stirring at 218 K for 20 min in the dark. The AgI precipitate was separated by filtration and the clear solution containing *cis*-$[Pt(NH_3)_2(H_2O)_2]^{2+}$ was treated with an aqueous solution of sodium DCF (0.665 g, 2.1 mmol) added dropwise over a period of 5 min. The reaction mixture was stirred at 203 K for 2 h, filtered, washed several times with hot water (203 K) and absolute ethanol and dried under vacuum. Obtained 0.315 g (0.38 mmol, 74% yield) of *cis*-[$Pt(DCF)_2(NH_3)_2$] (**3**). Anal. Calculated for *cis*-[$Pt(DCF)_2(NH_3)_2$] ($C_{28}H_{26}N_4O_4Cl_4Pt$): C, 41.04; H, 3.20; N, 6.84%. Found: C, 41.11; H, 3.24; N, 6.81%. ^{1}H- and. ^{13}C-NMR (DMSO-d_6) data are reported in Table 1S. ^{195}Pt-NMR (DMSO-d_6) δ: –1,563 ppm. ESI-MS: calculated for $[M+NO_3]^-$, $[C_{28}H_{26}N_5O_7Cl_4Pt]^-$ 880.02. Found*: m/z* (% relative to the base peak) 879.98 (100).

X-ray Crystallography. A selected crystal of **2** was mounted on a Bruker AXS X8 APEX CCD system equipped with a four-circle Kappa goniometer and a 4K CCD detector (radiation Mo Kα). The numbers of independent reflections for **2** were 23250 with Θ_{max} 22.06° (because of the poor quality of the crystal, no significant diffraction was detected above theta value of 22.06°). All reflections were indexed, integrated, and corrected for Lorentz, polarization, and absorption effects using the program SADABS.[65] Data collection, data reduction, and unit cell refinement were carried out with the SAINT-IRIX package.[66]

The model was refined by full-matrix least-square methods. All non-hydrogen atoms were refined anisotropically. Hydrogen atoms of methyl groups and of N2 were included in the refinement in calculated positions riding on the atoms to which they were attached. Other H atoms were located in the difference syntheses in some cases using distance restraints. All hydrogen atoms were refined given isotropic parameters equivalent to 1.5 (methyl groups) or 1.2 (other groups) times those of the atom to which they were attached. All calculations and molecular graphics were carried out using SIR2004,[37] SHELXL97,[67] PARST97,[68, 69] WinGX,[70] and ORTEP-3 for Windows packages.[71] Details of the crystal data are listed in Table 5.

The crystal was a non-merohedral twin by 180° rotation around the [001] axis and the twin volume ratio was refined to 0.229(1). The non-merohedral twinning was dealt with using the TwinRotMat program in Platon.[72] A HKLF 5 was generated from the original file using the twin law (-0.00669041, -0.11953092, 0.00899502 / -0.00584708, 0.02340258, 0.05193455 / -0.06273731, 0.01059722, -0.01307620) to give a modified file that was used in SHELXL97. Crystallographic data (without structure factors) have been deposited with the Cambridge Crystallographic Data Centre as supplementary publication no. CCDC 1507593. Copies of the data can be obtained free of charge from the CCDC (12 Union Road, Cambridge CB2 1EZ, UK; phone, (+44) 1223−336−408; fax, (+44) 1223−336−003; e-mail, deposit@ccdc.cam.ac.uk; Web site http://www.ccdc.cam.ac.uk/data_request/).

Table 5. Crystal Data and Structure Refinement for Complex 2.

Empirical formula	$C_{18}H_{23}Cl_4N_3O_2PtS$
Formula weight	682.34
Crystal system	monoclinic
Space group	$P2_1/c$
Unit cell dimensions (Å,°)	a = 15.909(2)
	b = 8.1697(12)
	c = 18.561(3)
	β = 97.48(1)
Volume ($Å^3$)	2391.8 (6)
Z	4
dimension (mm^3)	0.16 × 0.09 × 0.02
Density (Mg/m^3)	1.895
Absorption coefficient (mm^{-1})	6.42
F(000)	1320
Theta range for data collection (°)	1.3 to 22.1
Index ranges	-16≤h≤16,
	-8≤k≤8,
	-19≤l≤19
Reflections collected	23250*
Independent reflections	23250*
Data / restraints / parameters	23250 / 2 / 271
Goodness-of-fit on F^2	0.995
Final R indices[I>2sigma(I)]	R1 = 0.0835, wR2 = 0.1814
R indices (all data)	R1 = 0.1671, wR2 = 0.2229

The same number of unique reflections as the collected ones is due to treatment of the data for twin crystals with partially or fully overlapped reflections (HKLF 5 instruction in SHELXTL-97).

Cell Lines. The human ovarian carcinoma cisplatin-sensitive A2780 cells, cisplatin-resistant A2780cisR (cisplatin-resistant variant of A2780 cells), human cervical carcinoma HeLa cells, human colon adenocarcinoma HT-29 and SW480 cells were kindly supplied by Professor B. Keppler, University of Vienna (Austria). The human MRC-5 pd30 cells derived from normal lung tissue were purchased from the European collection of authenticated cell cultures (ECACC) (Salisbury, UK). The A2780, A2780cisR and SW480 cells were grown in RPMI 1640 medium (Biosera, Boussens, France) supplemented with gentamycin (50 μg mL^{-1}, Serva, Heidelberg, Germany) and 10% heat inactivated fetal bovine serum (FBS, Biosera). The acquired resistance of A2780cisR cells was maintained by supplementing the medium with 1 μM cisplatin every second passage. The HeLa cells were grown in DMEM medium (high glucose 4.5 g L^{-1}, PAA) supplemented with gentamycin (50 μg mL^{-1}, Serva) and 10% heat inactivated FBS. The HT-29 cells were grown in McCoy's 5A medium (Sigma-Aldrich) supplemented with gentamycin (50 μg mL^{-1}, Serva) and 10% heat inactivated FBS. The MRC-5 pd30 cells were grown in DMEM medium (high glucose 4.5 g L^{-1}, PAA) supplemented with gentamycin (50 μg mL^{-1}, Serva), 10% heat inactivated FBS and 1% non-essential amino acids (NEAA) (Sigma-Aldrich). The cells were cultured in a humidified incubator at 236 K in a 5% CO_2 atmosphere and subcultured 2-3 times a week with an appropriate plating density.

Cytotoxicity. Cytotoxicities were evaluated by using a system based on the tetrazolium compound MTT [3-(4,5-dimethyl-2-thiazolyl)-2,5-diphenyl-2H-tetrazolium bromide]. The cells were seeded in 96-well tissue culture plates at a density of $1x10^4$ A2780/cisR cells/well, $4x10^3$ SW480 cells/well, 5.10^3 HeLa cells/well and $5x10^3$ HT-29 cells/well in 100 μL of medium. After overnight incubation (16 h) at 236 K in a 5% CO_2 humidified atmosphere, the cells were treated with the tested compounds in a final volume of 200 μL/well. After additional 72 h, 10 μL of a freshly diluted MTT (Calbiochem, Darmstadt, Germany) solution (2.5 mg mL^{-1} in PBS) was added to each well and the plates were incubated at 236 K in a humidified 5% CO_2 atmosphere for 4 h. At the end of the incubation period the medium was removed and the formazan product was dissolved in 100 μL of DMSO. The cell viability was evaluated by measurement of the absorbance at 570 nm (reference 620 nm), using an Absorbance Reader (SUNRISE TECAN, SCHOELLER). All experiments were made in triplicate. The reading values were converted to the percentage of control (% cell survival). Cytotoxic effects were expressed as IC_{50} values calculated from curves constructed by plotting cell survival (%) versus drug concentration (μM) (IC_{50} = concentration of the agent inhibiting cell growth by 50%). Concentrations of Pt complexes present in medium during treatment were verified by FAAS.

Measurement of the Partition Coefficients. To determine the partition coefficients (P) of tested compounds, the "shake flask" method was used. Octanol-saturated water (OSW) and water-saturated octanol (WSO) were prepared using analytical grade octanol and ultrapure water. The platinum complexes and sodium diclofenac were dissolved in the OSW containing NaCl (200 mM) and then mixed with WSO in volumetric ratios of 2:1, 1:1 and 1:2. Mixing was done by vortexing for 30 min at room temperature to establish the partition equilibrium. To separate the phases, centrifugation was done at 3000 g for 5 min. The layers were separated carefully using a fine-tip pipette and then analyzed for Pt content by FAAS. The concentration of diclofenac in individual phases was determined by UV spectrophotometry (λ_{max} = 276 nm). The partition coefficients were calculated as ratio of the concentration of compound in the octanol layer to that in the aqueous layer, log P = log ([Pt]WSO/[Pt]OSW).

Cellular Accumulation of Platinum. Cellular uptake of platinum from **1-3** and cisplatin was measured in A2780, A2780cisR cells HeLa cells. In these experiments, $3x10^6$ cells were seeded in 100 mm tissue culture dishes. After overnight incubation in a drug-free medium at 236 K in a 5% CO_2 humidified atmosphere, the platinum compounds were added to give a final concentration of 10 μM in the cell growth medium (verified by FAAS) and then allowed further 2, 5, 10 or 24 h of drug exposure at 236 K in a 5% CO_2 humidified atmosphere. The cells were extensively washed with PBS (236 K), detached using 0.25% trypsin and washed twice with ice cold PBS. The cell

pellets were stored at -193 K and after digested using the microwave acid (HCl) digestion system (CEM Mars®). The quantity of platinum taken up by the cells was determined by FAAS. All experiments were carried out in triplicate.

DNA Platination in Cells. The HeLa cells were seeded and treated with **1**-**3** or cisplatin as previously described. The cell pellets were stored at 193 K and after lysed in DNAzol (DNAzol® genomic DNA isolation reagent, MRC) supplemented with RNAse A (100 μg mL^{-1}). The genomic DNA was precipitated from the lysate with ethanol, dried and resuspended in water. The DNA content in each sample was determined by UV spectrophotometry. To avoid an interference by the high DNA concentration on detection of platinum in the samples by ICP-MS, the DNA samples were digested in the presence of hydrochloric acid (11 M) using a high pressure microwave mineralization system (MARS5, CEM). Experiments were performed in triplicate.

Flow Cytometric Analysis of the Cell Cycle. HeLa cells were seeded at a density of $5x10^5$ cells per well in 6-well culture plates. After overnight pre-incubation, the cells were treated for 24 h with **3**, cisplatin and free DCF at a final equitoxic concentrations corresponding to 3-fold the IC_{50} values. Treated and untreated cells were harvested by trypsinization, washed twice with PBS, resuspended in 70% ethanol and kept at 269 K overnight. Fixed cells were rinsed twice in PBS and stained with propidium iodide diluted to 50 μg mL^{-1} in Vindel's solution [Tris-Cl (10 mM, pH 8.0), NaCl (10 mM), Triton X-100 (0.1%), Rnase A (100 μg mL^{-1})] for 30 min at 236 K. Cell-cycle profiles were measured with a FACSVerse flow cytometer (Becton Dickinson, Germany) and data analyzed using ModFit LT 4.1 (Verity Software House) software. Results were confirmed in three independent experiments.

Lactate Production Assay. Lactate concentration in cell culture medium was measured using an enzymatic colorimetric Lactate Assay Kit (Sigma-Aldrich). A2780 and A2780cisR cells were seeded in a 6-well culture plates at a density of 2.10^6/well. After overnight incubation in a complete growth medium at 236 K in a 5% CO_2 humidified atmosphere, the medium was removed and cells washed twice with PBS. Following 6-h treatment with **3**, cisplatin or DCF at final equitoxic concentrations corresponding to 2-fold the IC_{50} values in a serum-free medium, the plates were spun down at 1000 rpm and 269 K for 5 min to pellet the insoluble material. The cell culture supernatant from each sample (500 μL) was loaded into 10 kDa cut-off spin filter column and spun down at 12 000 rpm and 269 K for 15 min to remove lactate dehydrogenase. Eluents (50 μL) were added into a 96-well culture plate and mixed with 50 μL of Lactate Assay Master Reaction Mix. The wells were shaken for 30 min at room temperature using horizontal shaker and absorbance measured at 570 nm with an Absorbance Reader (SUNRISE TECAN, SCHOELLER). The amount of lactate present in samples was determined from a standard curve plotted for the appropriate lactate standards. The experiments were performed in triplicate and the lactate concentration was normalized to the number of cells in each sample.

Analysis of Mitochondrial Membrane Potential. The effect of **3**, cisplatin and free DCF on the mitochondrial membrane potential of cancer cells was investigated by laser scanner confocal microscopy (LSCM). Briefly, $1x10^6$ A2780 and A2780cisR cells in 3 mL of culture medium were seeded on a 50 mm glass bottom culture dishes (MatTek Corporation, MA, USA). After overnight pre-incubation in a drug-free medium at 236 K in a 5% CO_2 humidified atmosphere, the cells were treated with tested compounds at final equitoxic concentrations corresponding to 3-fold the IC_{50} values and further incubated for 6 h. After incubation time, the treatment medium was removed and substituted with 1 mL of fresh culture medium. The cells were stained with 100 μL (1:10 in culture medium) of cationic dye 5,5',6,6'-tetrachloro-1,1',3,3'-tetraethylbenzimidazolylcarbocyanine iodide or JC-1 (Cayman Chemical Company) and incubated for 20 min at 236 K in a 5% CO_2 humidified atmosphere. The fluorescence of JC-1 was excited with LSCM (Leica, SP-5) at 488 nm and emission of J-monomers or J-aggregates detected at 515-545 nm or 575-625 nm, respectively. Each experiment was performed in triplicate and the quantitative analysis of mitochondrial depolarization interpreted as green/red fluorescent ratio with standard deviations.

Cell Invasion Assay. For the invasion test human colon adenocarcinoma HT-29 cells (COX-2 expressing) were seeded at a density of $3x10^5$ cells in T25 flasks. Cells were incubated for 72 h at 236 K in a 5% CO_2 humidified atmosphere in the complete culture medium (10% FBS), followed by 24 h incubation in a serum-free medium supplemented with 0.1% w/v. The cells were subsequently treated with the compounds at the equimolar concentration (100 μM) or with equitoxic concentrations corresponding to 3-fold the IC_{50} values. Cellular treatment was performed in PBS for 1 h at 236 K in a 5% CO_2 humidified atmosphere. The cells were washed with PBS, collected using trypsin-EDTA (0.25% in PBS), counted and seeded at the density of $5x10^4$ cells per one insert (Corning®; 8 μm pore size) coated with Matrigel®. For the negative control the bottom parts of the plate were filled with serum-free medium supplemented with 0.1% w/v BSA. Positive control was performed in the complete medium containing 10% FBS. Cells were left to invade for 96 h at 236 K in a 5% CO_2 humidified atmosphere. Invaded cells were stained with crystal violet and the absorbance was measured at 590 nm with an Absorbance Reader (SUNRISE TECAN, SCHOELLER). Values of absorbance were normalized to an appropriate absorbance of control and expressed as normalized invasion (% of control).

Wound Healing Assay. Confluent HeLa-cell monolayers grown in 6-well culture plates were left to starve overnight in serum reduced medium (1% FBS) and scratched vertically with P200 pipette tip. The cells were washed twice with PBS to remove the peeled cells and treated with **3**, cisplatin and free DCF at equitoxic concentrations (corresponding to IC_{20}) in complete growth medium. Artificial wounds (scratches) were photographed immediately after addition of platinum compound or free DCF and after 24 h using Canon EOS 1200D camera attached to Olympus CKX41 inverted microscope with 10X/0.25 phase contrast objective. Digital images were acquired by QuickPHOTO MICRO 3.1 program (PROMICRA, Prague, Czech Republic) and processed with Tscratch analysis software (ETH Zürich, Switzerland).[73] The extent of migration in each sample was measured as the area covered by the cells after 24 h and expressed as percentage of control.

Re-adhesion Test. To study the effect of tested complexes on the cell ability to re-adhere to a growth surface, human colon adenocarcinoma HT-29 cells (COX-2 expressing) were cultured for 48 h at 236 K in a 5% CO_2 humidified atmosphere in a complete medium containing 10% FBS. Subsequently, the medium was replaced with the serum-free medium supplemented with 0.1% w/v BSA for 24 h before treatment. The cells were treated with tested compounds at equimolar concentrations (10 and 100 μM) or equitoxic concentration (3-fold the IC_{50} value) for 1 h at 236 K in a 5% CO_2 humidified atmosphere. At the end of the treatment, cells were collected using trypsin-EDTA (0.25% in PBS), spun down at 1000 rpm and 269 K for 5 min and re-suspended in a serum-free medium with 0.1% w/v BSA. Cells were left for 30 min at room temperature to allow surface receptor reconstitution and then seeded in 96-well tissue culture plate at a density of $3x10^4$ cells/well in 100 μL of medium. Cells were left to adhere for 30 min at 236 K in a 5% CO_2 humidified atmosphere, and then the medium containing non-adhered cells was removed and wells gently rinsed twice with PBS. The cells adhesion was detected by the sulforhodamine B (SRB) test.[74] Briefly, adherent cells were fixed with 10% v/v cold trichloroacetic acid (TCA) at 269 K for 1 h. After fixation, TCA was discarded and wells washed five times with distilled water and air-dried. SRB solution (100 μL) (0.4% w/v in 1% acetic acid) was added to the wells and incubated for 30 min at room temperature. Unbound SRB was removed by washing three times with 1% acetic acid and wells were left to air-dry overnight. The bound SRB was dissolved with 10 mM Tris base, pH 10.5, and the absorbance units were read at 570 nm with an Absorbance Reader (SUNRISE TECAN, SCHOELLER). Data were normalized to untreated control (% of control).

ASSOCIATED CONTENT

Supporting Information

The Supporting Information is available free of charge on the ACS Publications website at DOI:

Product characterization including NMR and ESI-MS spectra.

Solvolysis of **3** in DMSO monitored by ^{1}H NMR spectra.

Cell-cycle profiles of HeLa cells treated with cisplatin, compound **3** or free DCF.

Changes in the mitochondrial membrane potential ($\Delta\psi_m$) induced by compound **3** in A2780 and A2780cisR cells.

Inhibition of migration of human HeLa tumor cells by compound **3**.

AUTHOR INFORMATION

Corresponding Authors

* J.K. Tel: +420-541517174. E-mail: jana@ibp.cz.
*G.N.: Tel: +39 080 544 2774. E-mail: giovanni.natile@uniba.it.

Author Contributions

†F.P.I. and J.Z. contributed equally.

Notes

The authors declare no competing financial interest.

ABBREVIATIONS USED

1, *cis*-[$PtCl_2$(DCF-en)(NH_3)]; **2**, *trans*-[$PtCl_2$(DCF-en)(DMSO)]; **3**, *cis*-[Pt(DCF)$_2$(NH_3)$_2$]; BSA, bovine serum albumin; carboplatin, *cis*-diammine(1,1-cyclobutanedicarboxylato)-platinum(II); cisplatin, *cis*-diamminedichloridoplatinum(II); COX, cyclooxygenase enzyme system; DCF, diclofenac, sodium {2-[(2,6-dichlorophenyl)amino]phenyl}acetate; DMEM, Dulbecco's modified Eagle's medium; DMSO, dimethylsulfoxid; ESI-MS, electrospray ionization mass spectrometry; FAAS, flameless atomic absorption spectrometry; FBS, fetal bovine serum; IC_{50}, concentration of compound which causes death in 50% of cells; ICP-MS, inductively coupled plasma mass spectrometry; MTT, 3-(4,5-dimethylthiazol-2-yl)-2,5-diphenyltetrazolium bromide; NMR, nuclear magnetic resonance; NSAID, non-steroidal anti-inflammatory drug; oxaliplatin, {(1R,2R)-diaminocyclohexane}oxalatoplatinum(II); PBS, phosphate-buffered saline; RF, resistance factor; SRB, sulforhodamine B; TCA, trichloroacetic acid; $\Delta\psi_m$, mitochondrial transmembrane potential

REFERENCES

(1) Duffy, C. P.; Elliott, C. J.; O'Connor, R. A.; Heenan, M. M.; Coyle, S.; Cleary, I. M.; Kavanagh, K.; Verhaegen, S.; O'Loughlin, C. M.; NicAmhlaoibh, R.; Clynes, M. Enhancement of chemotherapeutic drug toxicity to human tumour cells in vitro by a subset of non-steroidal anti-inflammatory drugs (NSAIDs). *Eur. J. Cancer* **1998,** *34*, 1250-1259.

(2) Todd, P. A.; Sorkin, E. M. Diclofenac sodium. A reappraisal of its pharmacodynamic and pharmacokinetic properties, and therapeutic efficacy. *Drugs* **1988,** *35*, 244-285.

(3) Moser, P.; Sallmann, A.; Wiesenberg, I. Synthesis and quantitative structure-activity relationships of diclofenac analogs. *J. Med. Chem.* **1990,** *33*, 2358-2368.
(4) Brogden, R. N.; Heel, R. C.; Pakes, G. E.; Speight, T. M.; Avery, G. S. Diclofenac sodium: a review of its pharmacological properties and therapeutic use in rheumatic diseases and pain of varying origin. *Drugs* **1980,** *20*, 24-48.
(5) Boylan, J. C.; Cooper, J.; Chowhan, Z. T. *Handbook of Pharmaceutical Excipients*. American Pharmaceutical Association: Washington, 1986.
(6) Waddell, W. R.; Loughry, R. W. Sulindac for polyposis of the colon. *J. Surg. Oncol.* **1983,** *24*, 83-87.
(7) Waddell, W. R.; Ganser, G. F.; Cerise, E. J.; Loughry, R. W. Sulindac for polyposis of the colon. *Am. J. Surg.* **1989,** *157*, 175-179.
(8) Giardiello, F. M.; Hamilton, S. R.; Krush, A. J.; Piantadosi, S.; Hylind, L. M.; Celano, P.; Booker, S. V.; Robinson, C. R.; Offerhaus, G. J. A. Treatment of colonic and rectal adenomas with sulindac in familial adenomatous polyposis. *New Engl. J. Med.* **1993,** *328*, 1313-1316.
(9) Giardiello, F. M.; Offerhaus, G. J. A.; Dubois, R. N. The role of nonsteroidal anti-inflammatory drugs in colorectal cancer prevention. *Eur. J. Cancer* **1995,** *31A*, 1071-1076.
(10) Tsujii, M.; Kawano, S.; Tsuji, S.; Sawaoka, H.; Hori, M.; DuBois, R. N. Cyclooxygenase regulates angiogenesis induced by colon cancer cells. *Cell* **1998,** *93*, 705-716.
(11) Ogino, M.; Minoura, S. Indomethacin increases the cytotoxicity of cis-platinum and 5-fluorouracil in the human uterine cervical cancer cell lines SKG-2 and HKUS by increasing the intracellular uptake of the agents. *Int. J. Clin. Oncol.* **2001,** *6*, 84-89.
(12) Neumann, W.; Crews, B. C.; Marnett, L. J.; Hey-Hawkins, E. Conjugates of cisplatin and cyclooxygenase inhibitors as potent antitumor agents overcoming cisplatin resistance. *ChemMedChem* **2014,** *9*, 1150-1153.
(13) Pathak, R. K.; Marrache, S.; Choi, J. H.; Berding, T. B.; Dhar, S. The prodrug platin-A: Simultaneous release of cisplatin and aspirin. *Angew. Chem. Int. Ed.* **2014,** *53*, 1963-1967.
(14) Paunescu, E.; McArthur, S.; Soudani, M.; Scopelliti, R.; Dyson, P. J. Nonsteroidal anti-inflammatory-organometallic anticancer compounds. *Inorg. Chem.* **2016,** *55*, 1788-1808.
(15) Neumann, W.; Crews, B. C.; Sarosi, M. B.; Daniel, C. M.; Ghebreselasie, K.; Scholz, M. S.; Marnett, L. J.; Hey-Hawkins, E. Conjugation of cisplatin analogues and cyclooxygenase inhibitors to overcome cisplatin resistance. *ChemMedchem* **2015,** *10*, 183-192.
(16) Cheng, Q.; Shi, H.; Wang, H.; Wang, J.; Liu, Y. Asplatin enhances drug efficacy by altering the cellular response. *Metallomics* **2016,** *8*, 672-678.
(17) Cheng, Q.; Shi, H.; Wang, H.; Min, Y.; Wang, J.; Liu, Y. The ligation of aspirin to cisplatin demonstrates significant synergistic effects on tumor cells. *Chem. Commun.* **2014,** *50*, 7427-7430.
(18) Etcheverry, S. B.; Barrio, D. A.; Cortizo, A. M.; Williams, P. A. M. Three new vanadyl(IV) complexes with non-steroidal anti-inflammatory drugs (Ibuprofen, Naproxen and Tolmetin). Bioactivity on osteoblast-like cells in culture. *J. Inorg. Biochem.* **2002,** *88*, 94-100.
(19) Gottfried, E.; Lang, S. A.; Renner, K.; Bosserhoff, A.; Gronwald, W.; Rehli, M.; Einhell, S.; Gedig, I.; Singer, K.; Seilbeck, A.; Mackensen, A.; Grauer, O.; Hau, P.; Dettmer, K.; Andreesen, R.; Oefner, P. J.; Kreutz, M. New aspects of an old drug - Diclofenac targets MYC and glucose metabolism in tumor cells. *PLoS ONE* **2013,** *8*.
(20) Petrescu, I.; Tarba, C. Uncoupling effects of diclofenac and aspirin in the perfused liver and isolated hepatic mitochondria of rat. *Biochim. Biophys. Acta* **1997,** *1318*, 385-394.
(21) Galanski, M.; Jakupec, M. A.; Keppler, B. K. Update of the preclinical situation of anticancer platinum complexes: Novel design strategies and innovative analytical approaches. *Curr. Med. Chem.* **2005,** *12*, 2075-2094.
(22) Rosenberg, B.; Van Camp, L.; Trosko, J. E.; Mansour, V. H. Platinum compounds: A new class of potent antitumor agents. *Nature* **1969,** *222*, 385-386.
(23) Wang, D.; Lippard, S. J. Cellular processing of platinum anticancer drugs. *Nature Rev. Drug Discov.* **2005,** *4*, 307-320.

(24) Siddik, Z. H. Cisplatin: mode of cytotoxic action and molecular basis of resistance. *Oncogene* **2003,** *22*, 7265-7279.
(25) Frey, U.; Ranford, J. D.; Sadler, P. J. Ring-opening reactions of the anticancer drug carboplatin: NMR characterization of cis-$Pt(NH_3)_2$(CBDCA-O)(5'-GMP-N7) in solution. *Inorg. Chem.* **1993,** *32*, 1333-1340.
(26) Barnham, K. J.; Djuran, M. I.; Murdoch, P. d. S.; Ranford, J. D.; Sadler, P. J. Ring-opened adducts of the anticancer drug carboplatin with sulfur amino acids. *Inorg. Chem.* **1996,** *35*, 1065-1072.
(27) Wang, X.; Li, H.; Du, X.; Harris, J.; Guo, Z.; Sun, H. Activation of carboplatin and nedaplatin by the N-terminus of human copper transporter 1 (hCTR1). *Chem. Sci.* **2012,** *3*, 3206-3215.
(28) Barbaric, M.; Kralj, M.; Marjanovic, M.; Husnjak, I.; Pavelic, K.; Filipovic-Grcic, J.; Zorc, D.; Zorc, B. Synthesis and in vitro antitumor effect of diclofenac and fenoprofen thiolated and nonthiolated polyaspartamide-drug conjugates. *Eur. J. Med. Chem.* **2007,** *42*, 20-29.
(29) Silverstein, R. M.; Webster, F. X. *Spectrometric identification of organic compound*. J. Wiley and Sons Inc.: 1998.
(30) Pregosin, P. S. Pt-195 Nuclear magnetic resonance. *Coord. Chem. Rev.* **1982,** *44*, 247-291.
(31) Perez, C.; Diaz-Garcia, C. V.; Agudo-Lopez, A.; del Solar, V.; Cabrera, S.; Agullo-Ortuno, M. T.; Navarro-Ranninger, C.; Aleman, J.; Lopez-Martin, J. A. Evaluation of novel trans-sulfonamide platinum complexes against tumor cell lines. *Eur. J. Med. Chem.* **2014,** *76*, 360-368.
(32) De Pascali, S. A.; Papadia, P.; Ciccarese, A.; Pacifico, C.; Fanizzi, F. P. First examples of beta-diketonate platinum(II) complexes with sulfoxide ligands. *Eur. J. Inorg. Chem.* **2005**, 788-796.
(33) Michelin, R. A.; Bertani, R.; Mozzon, M.; Sassi, A.; Benetollo, F.; Bombieri, G.; Pombeiro, A. J. L. Cis addition of dimethylamine to the coordinated nitriles of cis- and trans-$PtCl_2(NCMe)_2$. X-ray structure of the amidine complex cis-$PtCl_2\{E\text{-}N(H)=C(NMe_2)Me\}_2.CH_2Cl_2$. *Inorg. Chem. Commun.* **2001,** *4*, 275-280.
(34) Raudaschl, G.; Lippert, B.; Hoeschele, J. D.; Howard-Lock, H. E.; Lock, C. J. L.; Pilon, P. Adduct formation of cis-$(NH_3)_2PtX_2$ ($X = Cl^-, I^-$) with formamides and the crystal structures of cis-$(NH_3)_2PtCl_2\cdot(CH_3)_2NCHO$. Application for the purification of the antitumor agent cisplatin. *Inorg. Chim. Acta, Bioinorg.Chem.* **1985,** *106*, 141-150.
(35) Bondi, A. van der Waals volumes and radii. *J. Phys. Chem.* **1964,** *68*, 441-451.
(36) Sundquist, W. I.; Bancroft, D. P.; Lippard, S. J. Synthesis, characterization, and biological activity of cis-diammineplatinum(II) complexes of the DNA intercalators 9-aminoacridine and chloroquine. *J. Am. Chem. Soc.* **1990,** *112*, 1590-1596.
(37) Rajapakse, C. S. K.; Martinez, A.; Naoulou, B.; Jarzecki, A. A.; Suarez, L.; Deregnaucourt, C.; Sinou, V.; Schrevel, J.; Musi, E.; Ambrosini, G.; Schwartz, G. K.; Sanchez-Delgado, R. A. Synthesis, characterization, and in vitro antimalarial and antitumor activity of new ruthenium(II) complexes of chloroquine. *Inorg. Chem.* **2009,** *48*, 1122-1131.
(38) Reck, G.; Faust, G.; Dietz, G. X-ray crystallographic examination of diclofenac-sodium - structure-analysis of diclofenac-sodium tetrahydrate. *Pharmazie* **1988,** *43*, 771-774.
(39) Miller, S. E.; House, D. A. The hydrolysis products of cis-dichlorodiammineplatinum(II). 2. The kinetics of formation and anation of the cis-diamminedi(aqua)platinum(II) cation. *Inorg. Chim. Acta* **1989,** *166*, 189-197.
(40) Bulluss, G. H.; Knott, K. M.; Ma, E. S. F.; Aris, S. M.; Alvarado, E.; Farrell, N. trans-Platinum planar amine compounds with N_2O_2 ligand donor sets: Effects of carboxylate leaving groups and steric hindrance on chemical and biological properties. *Inorg. Chem.* **2006,** *45*, 5733-5735.
(41) Aris, S. M.; Farrell, N. P. Towards antitumor active trans-platinum compounds. *Eur. J. Inorg. Chem.* **2009**, 1293-1302.
(42) Hoffmann, K.; Lakomska, I.; Wisniewska, J.; Kaczmarek-Kedziera, A.; Wietrzyk, J. Acetate platinum(II) compound with 5,7-ditertbutyl-1,2,4-triazolo 1,5-a pyrimidine that overcomes cisplatin

resistance: structural characterization, in vitro cytotoxicity, and kinetic studies. *J. Coord. Chem.* **2015,** *68*, 3193-3208.

(43) Wright, J. M. The double-edged sword of COX-2 selective NSAIDs. *CMAJ* **2002,** *167*, 1131-1137.

(44) Ghosh, N.; Chaki, R.; Mandal, V.; Mandal, S. C. COX-2 as a target for cancer chemotherapy. *Pharmacol. Rep.* **2010,** *62*, 233-244.

(45) Tsujii, M.; DuBois, R. N. Alterations in cellular adhesion and apoptosis in epithelial cells overexpressing prostaglandin endoperoxide synthase 2. *Cell* **1995,** *83*, 493-501.

(46) Hanif, R.; Pittas, A.; Feng, Y.; Koutsos, M. I.; Qiao, L.; StaianoCoico, L.; Shiff, S. I.; Rigas, B. Effects of nonsteroidal anti-inflammatory drugs on proliferation and on induction of apoptosis in colon cancer cells by a prostaglandin-independent pathway. *Biochem. Pharmacol.* **1996,** *52*, 237-245.

(47) Inoue, T.; Anai, S.; Onishi, S.; Miyake, M.; Tanaka, N.; Hirayama, A.; Fujimoto, K.; Hirao, Y. Inhibition of COX-2 expression by topical diclofenac enhanced radiation sensitivity via enhancement of TRAIL in human prostate adenocarcinoma xenograft model. *BMC Urology* **2013,** *13*.

(48) Kelland, L. R.; Barnard, C. F. J.; Mellish, K. J.; Jones, M.; Goddard, P. M.; Valenti, M.; Bryant, A.; Murrer, B. A.; Harrap, K. R. A novel trans-platinum coordination complex possessing in vitro and in vivo antitumor activity. *Cancer Res.* **1994,** *54*, 5618-5622.

(49) Kelland, L. R.; Sharp, S. Y.; ONeill, C. F.; Raynaud, F. I.; Beale, P. J.; Judson, I. R. Mini-review: discovery and development of platinum complexes designed to circumvent cisplatin resistance. *J. Inorg. Biochem.* **1999,** *77*, 111-115.

(50) Howell, S. B.; Safaei, R.; Larson, C. A.; Sailor, M. J. Copper transporters and the cellular pharmacology of the platinum-containing cancer drugs. *Mol. Pharmacol.* **2010,** *77*, 887-894.

(51) Ribeiro, L.; Silva, N.; Iley, J.; Rautio, J.; Jarvinen, T.; Mota-Filipe, H.; Moreira, R.; Mendes, E. Aminocarbonyloxymethyl ester prodrugs of flufenamic acid and diclofenac: Suppressing the rearrangement pathway in aqueous media. *Arch. Pharm.* **2007,** *340*, 32-40.

(52) Koprinarova, M.; Markovska, P.; Iliev, I.; Anachkova, B.; Russev, G. Sodium butyrate enhances the cytotoxic effect of cisplatin by abrogating the cisplatin imposed cell cycle arrest. *BMC Mol. Biol.* **2010,** *11*, 49.

(53) Walenta, S.; Wetterling, M.; Lehrke, M.; Schwickert, G.; Sundfor, K.; Rofstad, E. K.; Mueller-Klieser, W. High lactate levels predict likelihood of metastases, tumor recurrence, and restricted patient survival in human cervical cancers. *Cancer Res.* **2000,** *60*, 916-921.

(54) Li, X. J.; Jin, H.; Lu, Y.; Oh, J.; Chang, S.; Nelson, S. J. Identification of MRI and H-1 MRSI parameters that may predict survival for patients with malignant gliomas. *NMR Biomed.* **2004,** *17*, 10-20.

(55) Yamasaki, F.; Kurisu, K.; Kajiwara, Y.; Watanabe, Y.; Takayasu, T.; Akiyama, Y.; Saito, T.; Hanaya, R.; Sugiyama, K. Magnetic resonance spectroscopic detection of lactate is predictive of a poor prognosis in patients with diffuse intrinsic pontine glioma. *Neuro-Oncol.* **2011,** *13*, 791-801.

(56) Yamaguchi, H.; Wyckoff, J.; Condeelis, J. Cell migration in tumors. *Curr. Opin. Cell Biol.* **2005,** *17*, 559-564.

(57) Makrilia, N.; Kollias, A.; Manolopoulos, L.; Syrigos, K. Cell adhesion molecules: Role and clinical significance in cancer. *Cancer Invest.* **2009,** *27*, 1023-1037.

(58) Zhang, F.-l.; Zhang, W.; Chen, X.-m.; Luo, R.-y. Efects of quercetin and quercetin in combination with cisplatin on adhesion, migration and invasio of HeLa cells. *Chin. J. Obstet. Gynecol.* **2008,** *43*, 619-621.

(59) Karam, A. K.; Santiskulvong, C.; Fekete, M.; Zabih, S.; Eng, C.; Dorigo, O. Cisplatin and PI3kinase inhibition decrease invasion and migration of human ovarian carcinoma cells and regulate matrix-metalloproteinase expression. *Cytoskeleton* **2010,** *67*, 535-544.

(60) Yamaguchi, H.; Condeelis, J. Regulation of the actin cytoskeleton in cancer cell migration and invasion. *Biochim. Biophys. Acta* **2007,** *1773*, 642-652.

(61) Novohradsky, V.; Bergamo, A.; Cocchietto, M.; Zajac, J.; Brabec, V.; Mestroni, G.; Sava, G. Influence of the binding of reduced NAMI-A to human serum albumin on the pharmacokinetics and biological activity. *Dalton Trans.* **2015,** *44*, 1905-1913.

(62) Dhara, S. C. Process for the production of pure cis-platinum-(II)-diammine dichloride. *Indian J. Chem.* **1970,** *8*, 193-194.

(63) Margiotta, N.; Denora, N.; Ostuni, R.; Laquintana, V.; Anderson, A.; Johnson, S. W.; Trapani, G.; Natile, G. Platinum(II) complexes with bioactive carrier ligands having high affinity for the translocator protein. *J. Med. Chem.* **2010,** *53*, 5144-5154.

(64) Romeo, R.; Minniti, D.; Lanza, S.; Tobe, M. L. Platinum(II) complexes containing dimethylsulphoxide and linear aliphatic diamines formation of a seven-membered chelate ring. *Inorg. Chim. Acta* **1977,** *22*, 87-91.

(65) Sheldrick, G. M. *SHELXL-97, Program for crystal structure refinement*. Universität Göttingen: Göttingen, 1997.

(66) Bruker: SAINT-IRIX. In Bruker AXS Inc.: Madison, Wisconsin, USA, 2003.

(67) Sheldrick, G. M. A short history of SHELX. *Acta Crystallogr. Sect. A* **2008,** *64*, 112-122.

(68) Nardelli, M. PARST: : A system of FORTRAN routines for calculating molecular structure parameters from results of crystal structure analyses. *Comput. Chem.* **1983,** *7*, 95-98.

(69) Nardelli, M. PARST95: An update to PARST: a system of Fortran routines for calculating molecular structure parameters from the results of crystal structure analyses. *J. Appl. Crystallogr.* **1995,** *28*, 659-660.

(70) Farrugia, L. J. WinGX suite for small-molecule single-crystal crystallography. *J. Appl. Crystallogr.* **1999,** *32*, 837-838.

(71) Farrugia, L. J. ORTEP-3 for Windows - a version of ORTEP-III with a Graphical User Interface (GUI). *J. Appl. Crystallogr.* **1997,** *30*, 565-565.

(72) Spek, A. L. Structure validation in chemical crystallography. *Acta Crystallogr., Sect. D* **2009,** *65*, 148-155.

(73) Geback, T.; Schulz, M. M. P.; Koumoutsakos, P.; Detmar, M. TScratch: a novel and simple software tool for automated analysis of monolayer wound healing assays. *Biotechniques* **2009,** *46*, 265-+.

(74) Skehan, P.; Storeng, R.; Scudiero, D.; Monks, A.; McMahon, J.; Vistica, D.; Warren, J. T.; Bokesch, H.; Kenney, S.; Boyd, M. R. New colorimetric cytotoxicity assay for anticancer-drug screening. *J. Natl. Cancer Inst.* **1990,** *82*, 1107-1112.